GA–A25750

CHAPTER 4 — MATERIALS DEVELOPMENT FOR SULFUR-IODINE THERMOCHEMICAL HYDROGEN PRODUCTION

by
B. WONG and P.W. TRESTER

MARCH 2007

GENERAL ATOMICS

GA–A25750

CHAPTER 4 — MATERIALS DEVELOPMENT FOR SULFUR-IODINE THERMOCHEMICAL HYDROGEN PRODUCTION

by
B. WONG and P.W. TRESTER

This is a preprint of a chapter to be to be submitted for publication in *Materials for the Hydrogen Economy.*

GENERAL ATOMICS PROJECT 40017
MARCH 2007

GENERAL ATOMICS

TABLE OF CONTENTS

CONTENTS (Continued)

LIST OF FIGURES

LIST OF FIGURES (Continued)

LIST OF TABLES

LIST OF TABLES (Continued)

4. MATERIALS DEVELOPMENT FOR SULFUR-IODINE THERMOCHEMICAL HYDROGEN PRODUCTION

4.1. INTRODUCTION

The Sulfur-iodine (S-I) cycle is a thermochemical water-splitting process that utilizes thermal energy from a high-temperature heat source to produce hydrogen (H_2). It is comprised of three coupled chemical reactions as shown in Figure 4-1. First, the central low-temperature Bunsen reaction (Section I) is employed to produce two liquid phases from sulfur dioxide (SO_2), iodine (I_2) and water (H_2O). Under proper conditions, these two phases become immiscible and can be readily separated. The lighter upper phase is sulfuric acid (H_2SO_4) and the denser lower phase is an aqueous complex of HI, H_2O and I_2 (HI_x). After separation, the two liquid phases are sent to the two other sections for decomposition. Section II (H_2SO_4 decomposition) first concentrates the sulfuric acid that has been received from Section I and then decomposes it into SO_2, O_2 and H_2O at high temperature. The decomposed products are returned to Section I to continue the S-I cycle. In Section III (HI decomposition) HI is distilled from HI_x and is then decomposed into H_2 and I_2 at intermediate temperature. H_2 is separated for external use and iodine is cycled back to Section I to support the Bunsen reaction. The key advantages of the S-I cycle are that it has no effluent and the reactants are in easily transportable liquid or gaseous form. All the chemicals used are recycled and the only required process inputs are heat and water.

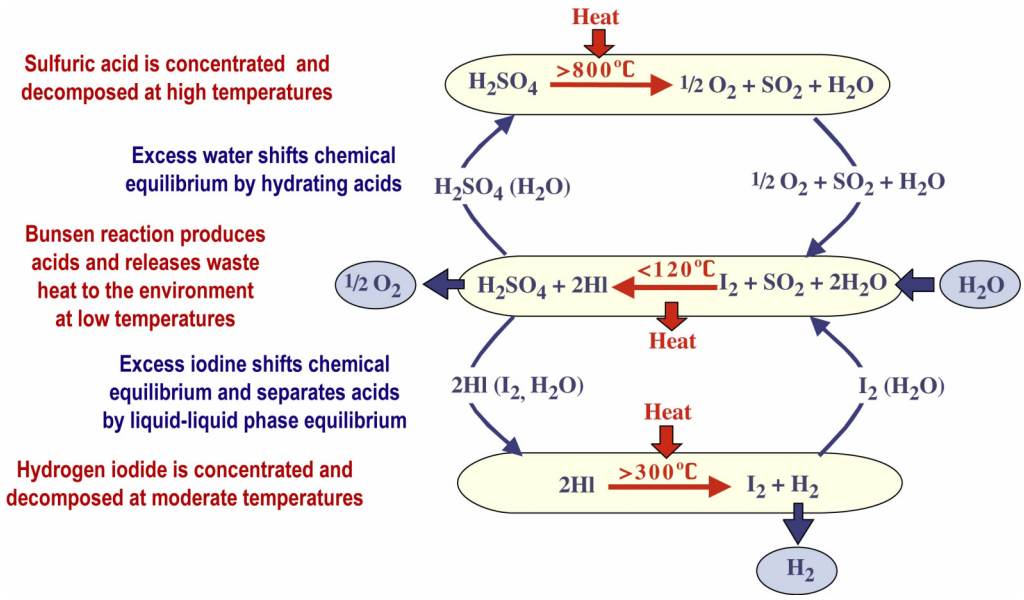

Fig. 4-1. The coupled chemical reactions of the S-I cycle.

Heat sources that are capable of delivering the high temperature required by H_2SO_4 decomposition reaction include the Modular Helium Reactor (MHR) [G11], a high Temperature Solar Tower and Coal and Natural Gas burning plants. Figure 4-2 shows a schematic of a conceptual S-I hydrogen plant design that is supported by the heat generated by a high-temperature nuclear reactor. The heat that is required to drive the two decomposition reactions and the electric turbine is delivered through an intermediate heat exchanger which employs helium gas as the heat transport medium. Other intermediate loop media such as molten fluoride salt have also been proposed for this application.

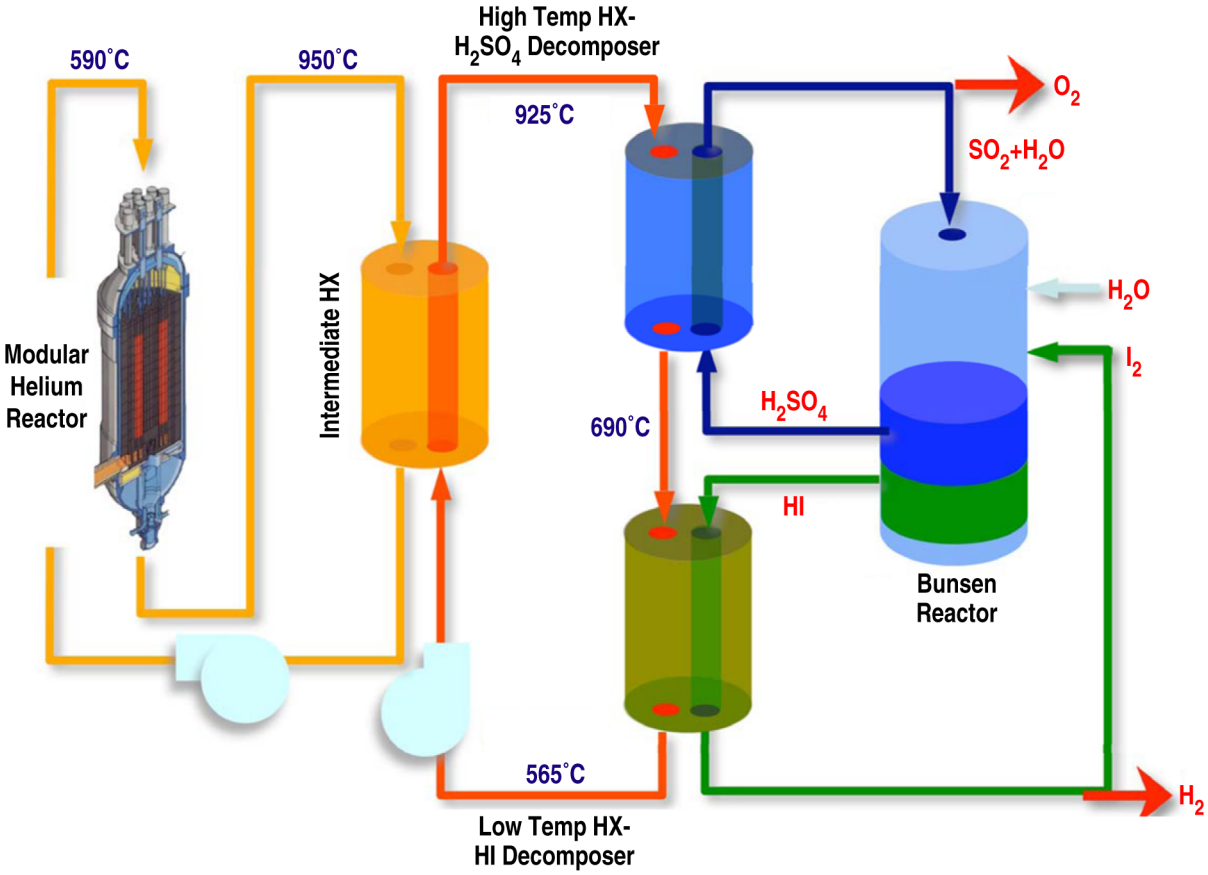

Fig. 4-2. A schematic for a nuclear-S-I hydrogen and electricity co-generation plant.

The S-I cycle is capable of achieving an energy efficiency of 50%, making it one of the most efficient cycles among all water splitting processes [G4,G23]. In addition, the S-I cycle is similar to other chemical production processes in that it is highly suitable to scaling up to large scale production of H_2, Hence, it has good potential to deliver large quantities of low cost hydrogen.

The baseline design for the current S-I work is the system configuration described in a report titled "High Efficiency Generation of Hydrogen Fuels Using Nuclear Power" [G1], which describes the equipment and component requirements in detail. Due to the chemicals involved and the high reaction temperatures, the S-I cycle presents a very corrosive working environment. In order to realize a safe, stable and functional hydrogen production plant, materials used to fabricate the boilers, heat exchangers and other components within each section must be carefully selected. The specific requirements will be determined by the process flowsheet for the individual section and the associated processing steps.

4.2. S-I CYCLE DEMONSTRATION

The S-I cycle was invented at General Atomics in the mid 1970s and was studied extensively in the US during the late 1970s and early 1980s [G2,G8,G9]. The chemical reactions within the different sections of the cycle were successfully demonstrated using glass apparatus. In addition, a high temperature metallic H_2SO_4 decomposition system was built and tested using the Solar Power Tower at the Georgia Institute of Technology in 1984 [G15]. The decomposition was successfully demonstrated with the aid of a solar heat source. For the past twenty years, researchers globally, especially those in Japan, have continued research and development on the cycle. Since 1988, a complete laboratory scale S-I test loop has been in operation in Japan by the Japan Atomic Energy Agency (JAEA). The system was constructed using glass equipment and is capable of delivering 30 ℓ/h of hydrogen [G12,G13].

To demonstrate the feasibility for large-scale hydrogen production, the US Department of Energy (DOE) Nuclear Hydrogen Initiative (NHI) is funding the construction of bench scale S-I loop that is fabricated with proper materials of construction (Figure 4-3). In addition to process demonstration, the materials and designs used in this integrated laboratory scale (ILS) loop are chosen so that they will be applicable to future scale up. This S-I loop is being constructed jointly by Commissariat à l'Énergie Atomique (CEA) – Section I, Sandia National Laboratory (SNL) – Section II and General Atomics (GA) – Section III. The three sections will be integrated for a bench scale demonstration capable of delivering 200–1000 ℓ/h of H_2 in 2008 [G1,G10].

4.3. S-I PROCESS FLOWSHEET

An extensive amount of flowsheet work has been performed to define the reaction conditions and process flow streams within the S-I cycle, which in turn determine the materials performance requirements. Advances in materials technology can re-define these flowsheets as better performing materials will allow the reactions to be conducted

more efficiently and extend component lifetime. This can lead to an increase in the overall cycle efficiency and reduce the cost of H_2 produced. It is, therefore, essential for one to be familiar with these flowsheets and understand the material performance requirements in order to develop and identify better construction materials.

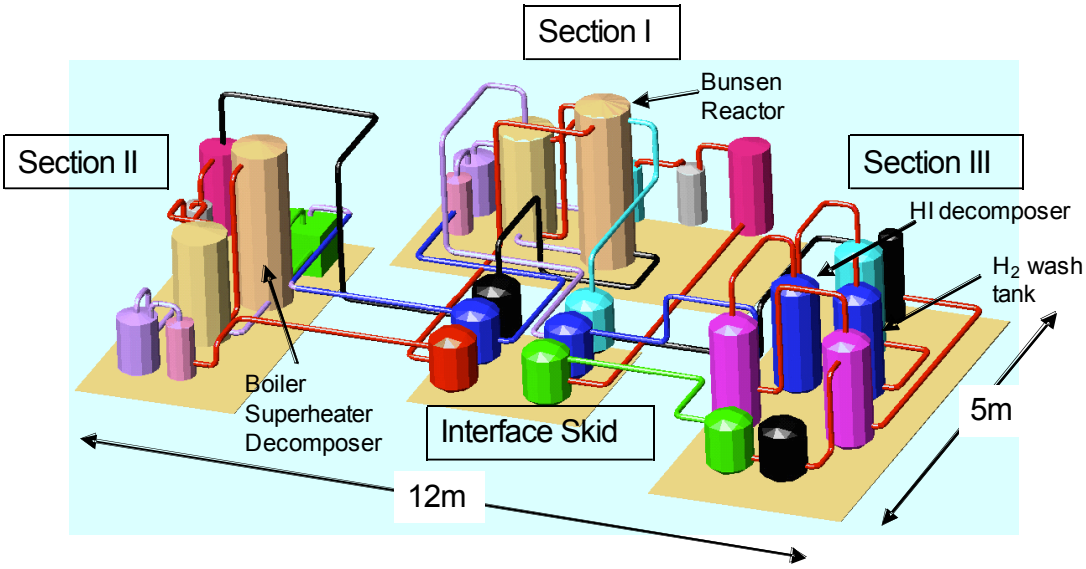

Fig. 4-3. A schematic of the sulfur-iodine integrated laboratory scale demonstration.

4.4. SECTION I — BUNSEN REACTION

Section I receives the recycled SO_2 gas from Section II and I_2 liquid from Section III are placed into contact with excess H_2O to promote a spontaneous reaction (Bunsen reaction) at 120°C. By adding excess I_2, the reaction products will form two immiscible liquid phases that can be separated via gravity [G9,G18]. The upper lighter phase is H_2SO_4 and the lower denser phase is an acid complex of HI, H_2O and I_2 (HI_x). This reaction is exothermic and if the reaction heat is not channeled away efficiently from the reactor, sulfur will form as a result of side reactions. Hence, the materials used to construct the reactor will need to be an efficient heat exchanger in addition to being corrosion resistant to the mixture of chemicals and gases that are present. There are four basic processing steps in this section (Figure 4-4) with the Bunsen Reaction being the key reaction. The associated process conditions are listed in Table 4-1.

Other than the main Bunsen reaction, the other three steps in this section involve separation of gases and H_2O from the flowing chemical stream. O_2, which forms as a result of water splitting, is removed from the recycled stream to avoid formation of complexes in the rest of the section. SO_2 is washed/separated from the Bunsen Reactor

output to prevent any side reaction down stream. The last step in Section I involves the extraction of H_2O from the HI_x product stream before it is sent to Section III. This will reduce the energy requirement as H_2O evaporation processes impose a high heat demand based on the current flowsheet. Hence, any reduction in H_2O content in the Bunsen reaction products will be beneficial to the overall cycle efficiency.

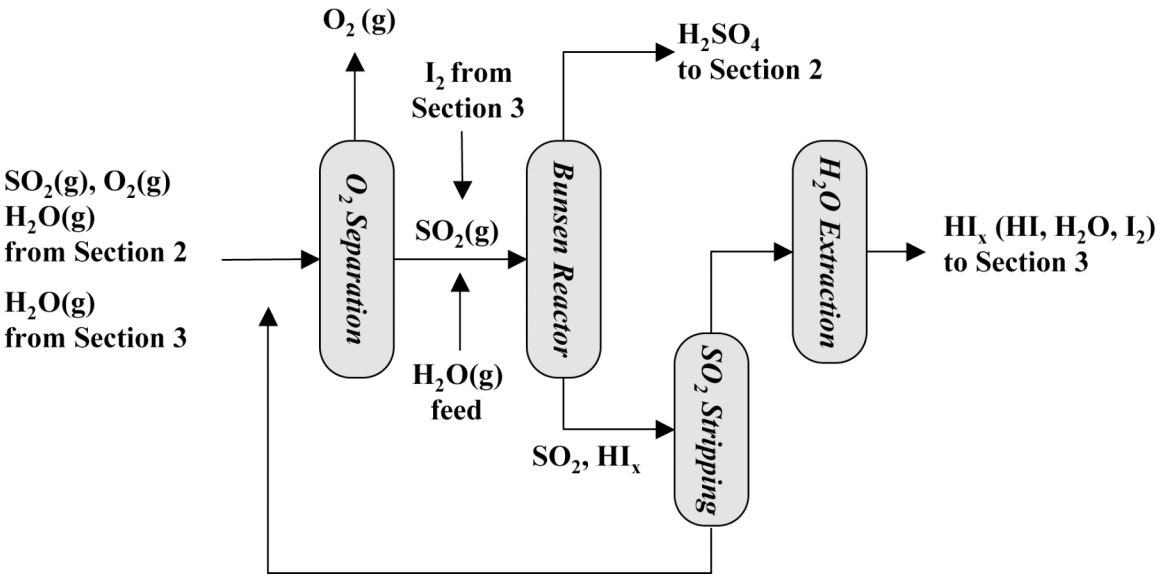

Fig. 4-4. Flowsheet for Section I (Bunsen reaction).

Table 4-1. Reaction Conditions for the Processing Steps in Section I

Reaction	Temp.	Pressure	Comments
O_2 separation	10°C	12 bar	• Condensation and wash of incoming stream • O_2 separation membrane
Bunsen reactor	120°C	10 bar	• HI_x – 13HI–9.5H_2O–77.5I_2 (wt%) • H_2SO_4 – 57 wt% • Phase separation by density • Heat exchanger (heat out) required
SO_2 stripping	120°C	1 bar	• H_2O wash • SO_2 separation membrane
H_2O extraction	120°C	1 bar	• Separation membrane • Electro-electro-dialysis

4.5. SECTION II — SULFURIC ACID DECOMPOSITION

This section receives H_2SO_4 from Section I and decomposes it into SO_2, O_2 and H_2O at high temperature. These gases are then returned to Section I (Figure 4-5) and SO_2 is used to support the Bunsen reaction. The decomposition is carried out in a number of steps under the conditions listed in Table 4-2. First, the incoming acid is concentrated from 57 wt% to 86 wt%. This is followed by pressurizing the acid stream to 70 bar to match the pressure of the He gas in the intermediate heat exchange loop. This will minimize the stress on the heat exchange interface and reduces creep effects at the high SO_3 decomposition temperature. The acid is heated up to around 475°C for vaporization. Starting at about 500°C, H_2SO_4 gas will begin to decompose into H_2O and SO_3. Further decomposition of SO_3 into SO_2 and O_2 is accomplished by a catalytic reaction at temperature around 850°C. Some flowsheet design has even proposed conducting the decomposition at 925°C to attain higher equilibrium conversion. This makes efficient heat conductivity an important material property.

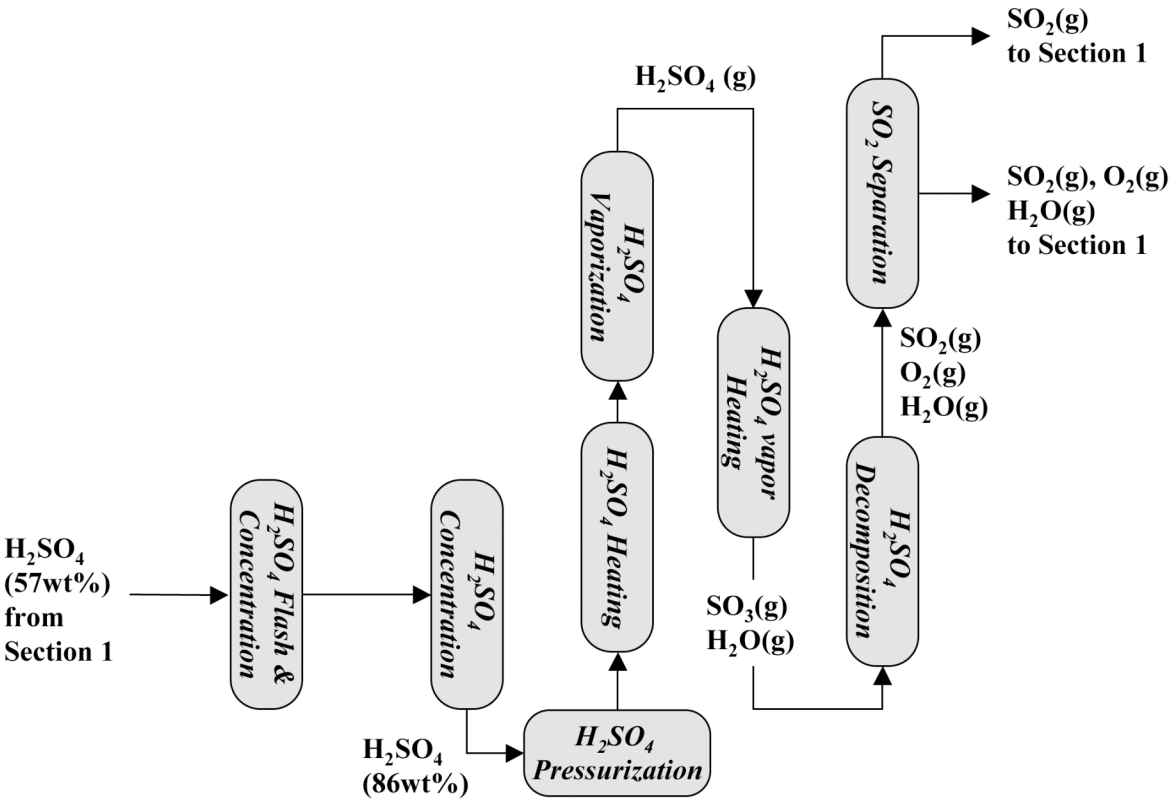

Fig. 4-5. Flowsheet for Section II (sulfuric acid decomposition).

Table 4-2. Reaction Conditions for the Processing Steps in Section II

Reactor	Temperature	Pressure	Comments
H_2SO_4 flash and concentration	120°C	1.85 → 0.1 bar	• H_2SO_4 (57 wt%)
H_2SO_4 concentration	120° → 170°C	0.1 bar	• H_2SO_4 (86wt%) • Heat exchanger (HX) (heat in) required
H_2SO_4 pressurization	170° → 175°C	0.1 → 70 bar	
H_2SO_4 heating	175° → 475°C	70 bar	• HX (heat in) required
H_2SO_4 vaporization	475° → 500°C	70 bar	• H_2SO_4 (86 wt%) • HX (heat in) required
H_2SO_4 heating	500° → 750°C	70 bar	• SO_3 formation • HX (heat in) required
H_2SO_4 decomposition	750° → 900°C	70 bar	• Catalytic reactor • HX (heat in) required
SO_2 separation	750° → 900°C	70 bar	• SO_2 membrane separator

Since $SO_3 \rightarrow SO_2 + O_2$ is an equilibrium reaction, one can enhance the reaction rate by removing SO_2 from the reactor. The only practical mean to accomplish this at the current decomposition temperature will be through the use of SO_2 selective permeable membrane. The lifetime permeability and structural integrity of such membrane at these operating temperatures are important issues that will need to be addressed.

4.6. SECTION III — HI DECOMPOSITION

This section receives HI_x from Section I for decomposition and produces H_2. Hydrogen iodide (HI) within the HI_x feed stream is distilled and decomposed into H_2 and I_2 and there are two alternatives to carry out this process: ***Extractive Distillation*** or ***Reactive Distillation***. The reaction conditions and the chemicals used in these two processes are different and their flowsheet will be addressed separately.

4.6.1. Extractive Distillation

Extractive distillation utilizes concentrated phosphoric acid (H_3PO_4) to extract HI and H_2O from HI_x as they, unlike I_2, are soluble in H_3PO_4. In addition, H_3PO_4 breaks the azeotrope between HI and H_2O thus permitting the distillation of HI from the acid

complex followed by decomposition [G2,G18]. A schematic of the process flowsheet and the corresponding reaction conditions are shown in Figure 4-6 and Table 4-3. There are four separate steps: 1) *iodine separation*, 2) *HI distillation*, 3) *phosphoric acid concentration* and 4) *gaseous HI decomposition*. In the iodine separation step, concentrated phosphoric acid (>96 wt%) is added to the HI_x feed from Section I and results in the formation a two phase liquid mixture of I_2 and HI + H_2O + H_3PO_4. The denser I_2 stream is separated by gravity and is returned to Section I to support the Bunsen reaction. The upper lighter HI – H_3PO_4 acid complex is sent to the distillation column to carry out HI distillation. HI gas is distilled from boiling HI + H_2O + H_3PO_4 and is passed on to the decomposition column for HI decomposition [HI(g) → H_2(g) + I_2(g)] in the presence of a catalyst. The decomposition can be carried out catalytically at either high temperature (~350°-450°C) in the gas phase or at low temperature (150°-300°C) in the liquid phase under pressure. At 450°C, the equilibrium conversion rate of HI into H_2 + I_2 is approximately 22%. Hence, removal of H_2 from the decomposition chamber can enhance the one-pass conversion rate and reduce the amount of HI that needs to be recycled through the decomposer. The phosphoric acid (H_3PO_4 + H_2O) which remains in the distillation column is concentrated from 87–96 wt% through a series of boilers via vacuum recompression (H_3PO_4 concentration). The concentrated acid is added to the incoming HI_x feed to anew the extraction process.

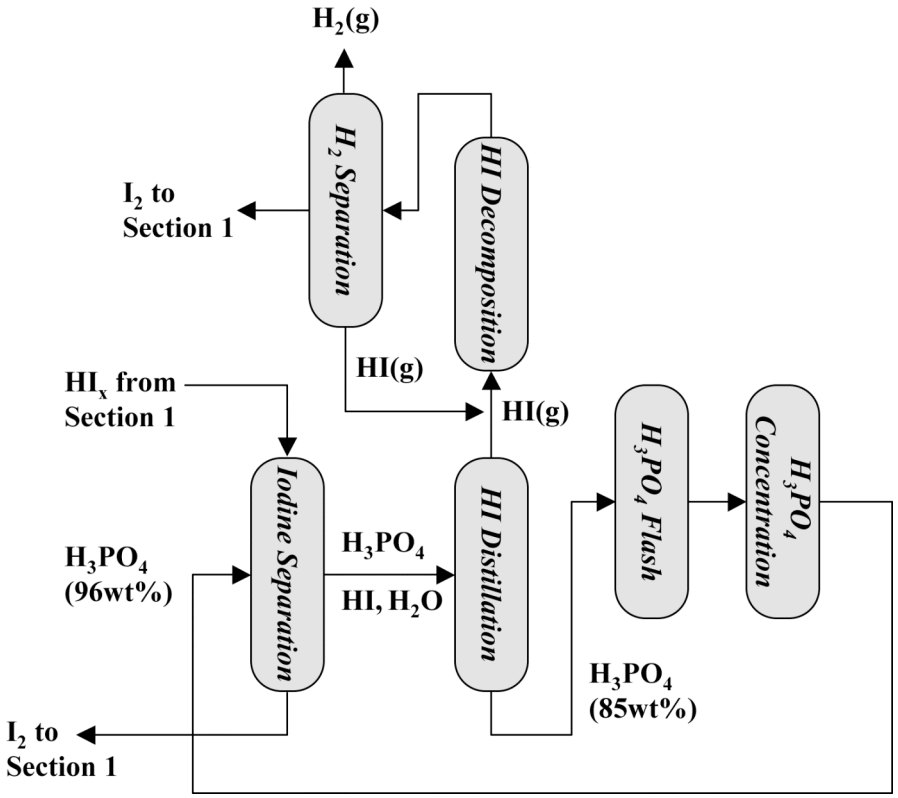

Fig. 4-6. Flowsheet for Section III (HI extractive distillation decomposition).

Table 4-3. Reaction Conditions for the Processing Steps in Section III Using Extractive Distillation

Reactor	Temperature	Pressure	Comments
I_2 separation	120°C	1 bar	• HI_x – 13HI–9.5H_2O–77.5I_2 (wt%) • H_3PO_4 (96 wt%)
HI distillation	120° → 170°C	1 bar	• Heat exchanger (HX) (heat in) required
HI decomposition	300° → 450°C	1 bar	• HI gas catalytic decomposition • HX (heat in) required
H_2 separation	<300°C	1 bar	• H_2O wash to separate trace HI • H_2 membrane separator
H_3PO_4 flash	160°C	1.0 → 0.1 bar	• H_3PO_4 acid (87 wt%)
H_3PO_4 concentration	165° → 220°C	0.1 bar	• 87 → 96 H_3PO_4 acid (wt%) • HX (heat in) required

4.6.2. Reactive Distillation

Reactive distillation is in theory a simpler process when compared to extractive distillation but it has yet to be demonstrated experimentally [G19]. There are two key differences between reactive and extractive distillation. First, unlike the extractive process, the HI_x azeotrope* is not broken so the composition in both the liquid and vapor phase is the same. Second, the reactive process must be conducted under pressure. Figure 4-7 shows a schematic of the reactive distillation flowsheet and the processing conditions are listed in Table 4-4. In this process, azeotropic HI_x is distilled inside a pressurized reactive column and the HI gas within the HI_x vapor stream is decomposed catalytically resulting in a gas mixture of HI, I_2, H_2 and H_2O. To accomplish this, the HI_x feed from Section I is first heated to 262°C from 120°C and is then fed into the reactive column. At the bottom of the column, the HI_x is brought to a boil at around 310°C and this boiling HI_x vapor results in an equilibrium vapor pressure of 750 psi inside the distillation column.

The distilled HI_x (HI, I_2 and H_2O) vapor flows through a bed of catalyst at the top half of the reactive column and HI within the vapor stream is decomposed into H_2 and I_2 gases at around 300°C. A condenser at the top of the reactive column condenses any un-reacted

*HI and H_2O form an azeotrope at 57wt% HI.

HI, I_2 and H_2O and the liquid is reflux back down the column. Consequently, the HI_x at the bottom of the reactive column is I_2 rich and is fed back to Section I as I_2 supply for the Bunsen reaction. H_2 is bled off the column top as a compressed gas for storage or use. The environment of HI_x, high temperature and high pressure required in the heat exchanger in the reactive distillation process makes it potentially one of the most corrosive environments within the S-I cycle.

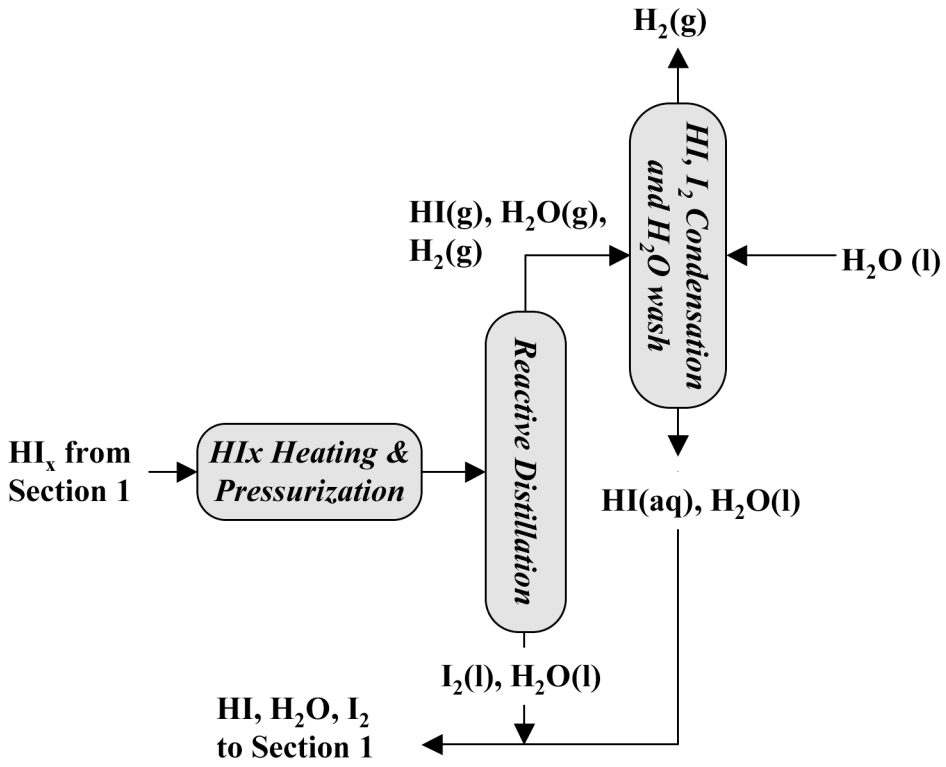

Fig. 4-7. Flowsheet for Section III (HI reactive distillation decomposition).

4.7. MATERIALS DEVELOPMENT FOR THE S-I CYCLE

There are three on going material research areas that are important for the eventual success of the S-I cycle. First and foremost is the development of construction materials that can handle the corrosive environment for the lifetime of the process equipment, especially heat exchangers, boilers and reactors. The other two areas involve gas permeable membrane and catalyst development. Identifying suitable membranes and reaction catalysts can improve the efficiency of the overall cycle and make H_2 production more economical. Effort is currently on going in all three disciplines to find the optimal material solutions.

Table 4-4. Reaction Conditions for the Main Reactions in Section III Using Reactive Distillation

Reactor	Temperature	Pressure	Comments
HI_x heating	120° → 260°C	1 → 50 bar	• HI_x – 13HI–9.5 H_2O–77.5I_2 (wt%) • Heat exchanger (HX) (heat in) required
Reactive distillation	310°C	50 bar	• HI_x gas phase catalytic decomposition • HX (heat in) required • Column bottom – 1.1HI–0.7H_2O–98.2I_2 (wt%)
HI, I_2 condensation	150°C	50 bar	

4.8. MATERIALS OF CONSTRUCTION

The general guidelines to selecting suitable construction materials for the S-I cycle can be summarized as follows:

- Materials must be resistant to the corrosive working environment,
- Materials used to build heat exchanger must have good thermal conductivity,
- Components manufactured from qualified materials must have suitable, mechanical and creep properties especially those operating at high temperatures,
- Metallic alloys materials must possess good hot and cold formability, weldability, and availability to make building of a hydrogen production plant practical,
- Materials components design should allow for non-destructive testing while they are being fabricated and when they are in service.

Using the above guidelines and the process conditions outlined in Tables 4-1 through 4-4, the following sections will review work pertaining to construction materials development for the S-I cycle.

4.9. MATERIALS OF CONSTRUCTION FOR SECTION I

The maximum temperature for the two corrosive acids in this section, HI_x and H_2SO_4, is 120°C. These two acids are also present in the other two sections but at higher temperatures. Liquid HI_x is used in Section III at temperatures up to 310°C and H_2SO_4 acid can be heated to 300°C and above during the concentration process in Section II. Based on conventional assumption that corrosion can be exponentially accelerated by an

increase in temperature, construction materials developed for use in the other sections will be applicable to the lower temperature environment in Section I or they can be the based line for future materials development. Hence, material development for Section I is limited at the present time.

To identify suitable materials for an acid complex such as HI_x, one can begin by surveying materials applicable to the individual acid/chemical. Tables 4-5 through 4-7 list the corrosion properties of various materials in I_2, HI acid and H_2SO_4. I_2 is a strong oxidizer, especially in liquid form at high temperature. The corrosion rate of a number of corrosion resistant materials in I_2 at 300°C and 450°C are listed in Table 4-5 [M15]. Even though the data shows that gold and platinum are stable in an I_2 environment, they have been found to dissolve in HI_x [M1]. Refractory metals such as Ta and Nb alloys are probably the best candidates within the I_2 rich environment in Section I.

Table 4-5. Corrosion Rate of Alloy in Pure Iodine at High Temperature

	Corrosion Rate (mils/yr)	
Alloy	**300°C**	**450°C**
Platinum	0.00	0.22
Tungsten	0.00	0.32
Gold	0.00	0.95
Molybdenum	0.12	1.30
Tantalum	0.16	34.66
Alloy B	2.24	18.12
Alloy 600	4.21	21.27

Table 4-6. Corrosion Rate of Alloy in HI Acid

Alloy	**Temperature (°C)**	**Corrosion Rate (mils/yr)**	**Comments**
Titanium	23	0.16	Conc. 57%
Niobium	<100	0.00	For all conc.
Gold	25	<0.04	Dilute
Palladium	25	65.73	
Zr_70_2	127	<0.04	Conc. 57 wt%

Table 4-7. Corrosion Test Results in ($50H_2SO_4$ + 0.1HI wt%) Solution at 120°C

	100 h Test		1000 h Test	
	I	II	I	II
Quartz glass	No change	0.20	No change	0.00
Silicon carbide	No change	2.95	No change	1.97
Silicon nitride	No change	3.35	No change	0.39
PFA		0.00	No change	0.00
PPS	No change	Weight gain	No change	+
Ta	No change	0.20	No change	0.00
Zr	No change	0.98	No change	0.00
Pb	No change	1.77	Roughened	1.97
Fe-15Si	Roughened	1.77		
Hastelloy C-276	Severely damaged	850.70		

HI is a strong reducing acid with a negative pH. Even though it is a common reagent in organic chemistry, corrosion data of materials in HI acid at elevated temperature is limited. Table 4-6 shows a summary of the available data [M14]. Noble and refractory metals have shown low corrosion rate but the temperatures at which the data was taken is lower than that in Bunsen reaction environment. The corrosion mechanism of H_2SO_4 depends on temperature and concentration. Within the Bunsen reactor environment, it is a reducing acid. Materials capable of containing H_2SO_4 will be considered in more details in the next section.

Based on the available data, construction materials for the Bunsen section will need to withstand a combination of reducing and oxidizing chemicals. Known for their performance under both reducing and oxidizing conditions, Ta and Nb refractory alloys can be suitable construction materials but comprehensive test data of these metals in an S-I environment is still lacking. Although the lower reaction temperatures of the Bunsen reaction will make corrosion less severe than in the other two sections, hydrogen embrittlement can become an issue at this temperature range.

In addition to metallic materials, ceramic such as SiC, Si_3N_4, Al_2O_3 and mullite are also materials that will most likely perform well under the harsh S-I environment and their applicability should be explored. Since the temperature does not exceed 120°C in the Section I, fluoro-polymer coatings such as teflon or glass-lined steel can also be viable options. The choices will depend more on the application.

The only corrosion experiment specifically designed for Section I was conducted by Trester, *et al.* [M14]. In it, they inserted welded rods of Zr_70_2 and Nb-1Zr into a glass liquid-phase separator within the Bunsen section. Borosilicate glass is resistant to these acids at this temperature. The immiscible gap at the HI_x and H_2SO_4 interface moved along the surface of the metal rods as the reaction progressed. Rapid localized corrosion was observed in Zr_70_2 whereas Nb-1Zr remained stable after a 4 h exposure at 105°C. Trester, *et al.* have also conducted an extensive corrosion study of materials in various composition of HI_x and it will be discussed in Section 4.11.1. More recent results from internal testing at General Atomics also showed that Zr705 corrodes rapidly in the HI_x – H_2SO_4 environment. Figure 4-8 shows a Zr705 coupon that has been immersed in a HI_x – H_2SO_4 static acid mixture. The test was conducted at 120°C for 450 h. Rapid corrosion of Zr705 in the area where it is in contact with HI_x has been observed.

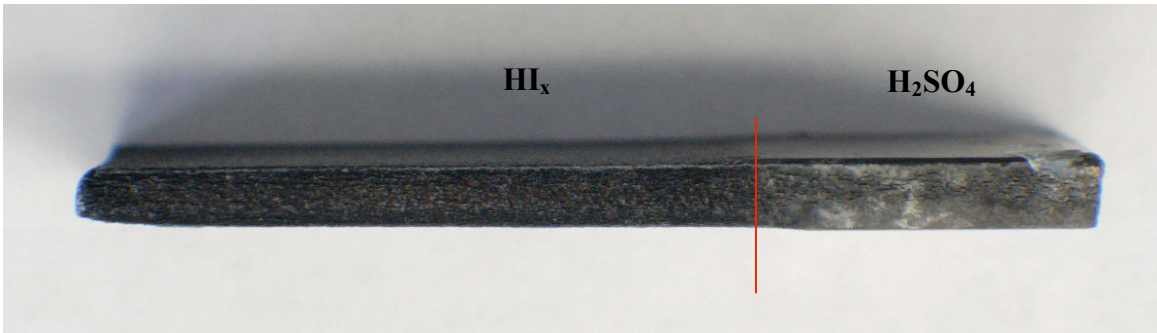

Fig. 4-8. Side view of a Zr_70_5 coupon tested in the static Bunsen separator acid (HI_x + H_2SO_4) for 450 h. The area that has been exposed to HI_x shows extensive dissolution.

Onuki, *et al.* [M6] have screened a number of materials in an acid mixture of H_2SO_4 (50 wt%) and HI (0.1 wt%) at temperatures up to 120°C (Table 4-7). This simulates the composition of the upper liquid phase. They found Ta, Zr, Pb and quartz glass to be corrosion resistant in this acid complex whereas common construction material such as stainless steel and Hastelloy did not possess acceptable corrosion rate. PFA (teflon) also showed satisfactory corrosion performance but I_2 absorption by PFA has been observed which raises question about its long-term viability.

From the currently available data, Ta, Nb and their alloys, glass-lined steel and probably SiC based materials are good candidates. They will need to undergo more extensive testing in the Bunsen reaction environment. Ta and SiC are good candidates for the reactor because of their good thermal conductivity but the final thermal properties requirements will depend on the heat exchanger design. The Bunsen section components for the bench scale S-I cycle demonstration experiment will be manufactured from glass lined steel since glass has been demonstrated to be inert to all the chemicals present, The

drawback is the uncertainty of the heat exchanging capability of such a construction to channel the heat away from the reactor.

4.10. MATERIALS OF CONSTRUCTION FOR SECTION II

The sulfuric acid decomposition reaction is divided into three different steps: ***concentration***, ***vaporization*** and ***decomposition***. Taking this into consideration, construction material requirements can be divided into two different categories. The first group consists of materials that can withstand the extreme corrosiveness of H_2SO_4 acid up to 450°C. The second group includes materials that have suitable high temperature (850°C) mechanical properties and good thermal conductivity that are also resistant to a gaseous oxidation and sulfidation environment.

In general, a liquid environment is much more corrosive than a gaseous environment due to a few factors. Ion transport, which is the driving force of all corrosion reactions, is much higher in the liquid phase thus enhancing the corrosion redox reaction. In a gaseous environment, the corrosion product will most likely stay on the reaction surface and may act as a barrier to decrease any further reaction. On the other hand, flowing liquid chemicals can dissolve and/or remove such corrosion product and lead to accelerated corrosion.

The step of H_2SO_4 concentration presents a very challenging corrosion problem. This is because the corrosion mechanism of liquid H_2SO_4 is linked to the temperature and the concentration of the acid. H_2SO_4 is reducing in nature when the acid concentration is below 85 wt% at room temperature or less than 65 wt% at higher temperatures. At high concentration and high temperature, it becomes an oxidizing agent. Hence, construction materials for the acid concentration application will face both the oxidizing and reducing conditions. Table 4-8 shows a summary of the materials that exhibit corrosion to the higher concentrations of H_2SO_4 [M15]. Ta and Au have low corrosion rate in higher concentration H_2SO_4 liquid phase environment. Precious metals such as Au and Pt have shown complete resistance at all concentrations of H_2SO_4. On the other hand, their inherent high cost and relatively low yield strength make them only viable as corrosion resistance coatings or cladding for components. Techniques to apply precious metals coating to a base structure are readily available but care must be taken to deal with inherent defects such as pinholes that can compromise the integrity of the component.

Table 4-8. Corrosion Rate of Alloy in Sulfuric Acid (wt%)

Alloy	Temperature (°C)	Corrosion Rate (mils/yr)	Comments
Inconel 625	80	90.19	Conc. 80%
Niobium	Boiling	50.02	60%
Gold	250	<1.97	For all conc.
316 stainless	93	4001.42	Conc. 80%
Tantalum	200	<0.04	Conc. 98%

Effort to develop materials for the H_2SO_4 concentration process has emphasized developing noble metals, engineering alloys and SiC based ceramics for H_2SO_4 concentration application [M1,M2,M5,M8,M10,M13]. For low temperature applications within the Section II process, Hastelloy B, Incoloy 825, Alloy 20, glass-lined and teflon lined and coated steel can be used as their behavior in H_2SO_4 is well documented.

Savitsky, *et al.* reported a Ni-Cr alloy (80Ni-15Cr-5Al) that has improved corrosion performance in 94 wt% boiling H_2SO_4 acid. The corrosion rate is about 4 mm/yr compared to 11 mm/yr for a Cr-Ni steel alloy (Fe-18Ni-18Cr-2Ti). However, they demonstrated that by using Cr^+, Ni^+ and Al^+, ion-implantation to alter the surface properties of the Cr-Ni steel alloy, they were able to reduce the corrosion rate by a factor of 3. This is an interesting technique that needs to be explored further.

The casting alloy Duriron (Fe-14.2-Si-0.8C wt%), with its high Si content, has been shown to be extremely resistant against concentrated H_2SO_4, but the brittle nature limits machinability, assembly and maintenance of components. In light of this, iron-based alloys with lower Si content (4-6 wt%) such as Saramet 23, Saramet 35 and ZeCor are being tested for this application. These alloys have good ductility and forming characteristics and can be joined by traditional means such as arc welding. Investigators at Idaho National Lab. have established a screening effort studying the applicability of these alloys and other materials to the H_2SO_4 concentration process. Figure 4-9 shows the corrosion rate of various engineering alloys tested in 96 wt% H_2SO_4 at 200°C. The initial corrosion rate is relatively high but is reduced with test time. This can be attributed to the formation of a Si-rich passivation layer on the alloy that slows the corrosion process and consequently retards the corrosion rate (Figure 4-10). When the test was conducted at 375°C, the corrosion rate has a similar trend but the Si-rich passivation layer grows at a faster rate due to the faster kinetics. The corrosion resistance of the tested alloys is thought to depend to a large extent on adherence of the Si-rich layer to the alloy substrate. This is especially true in a boiling H_2SO_4 acid environment. New experiments

will need to be conducted to probe the effect of long-term operation and process variations on the corrosion resistance of these candidate alloys.

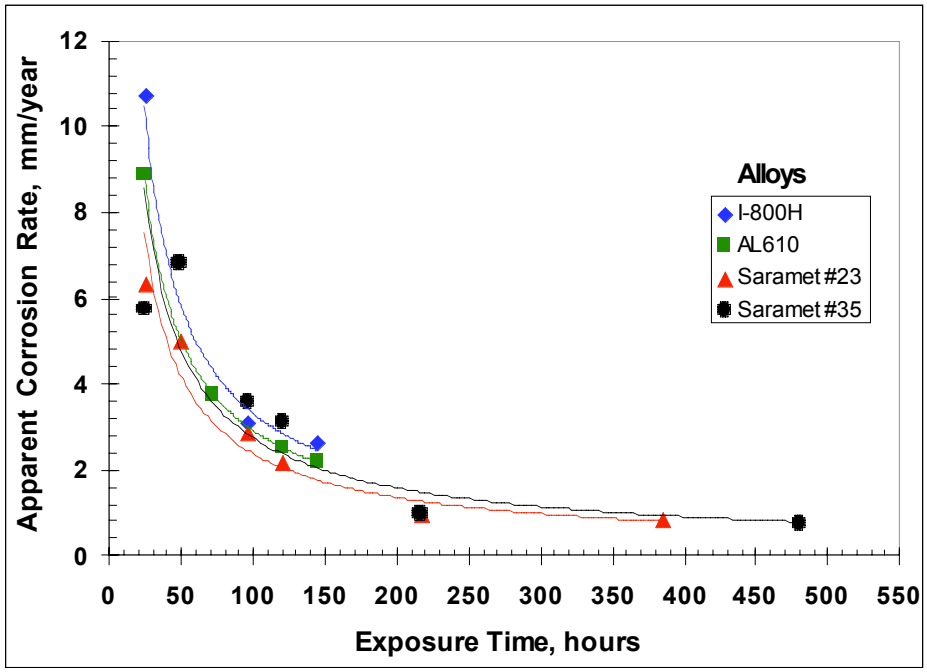

Fig. 4-9. Corrosion rate of selected alloy s as a function of exposure time. Conditions: 96wt% H_2SO_4 at 200°C and atmospheric pressure. (Plot courtesy of T. Lillo, Idaho National Lab.)

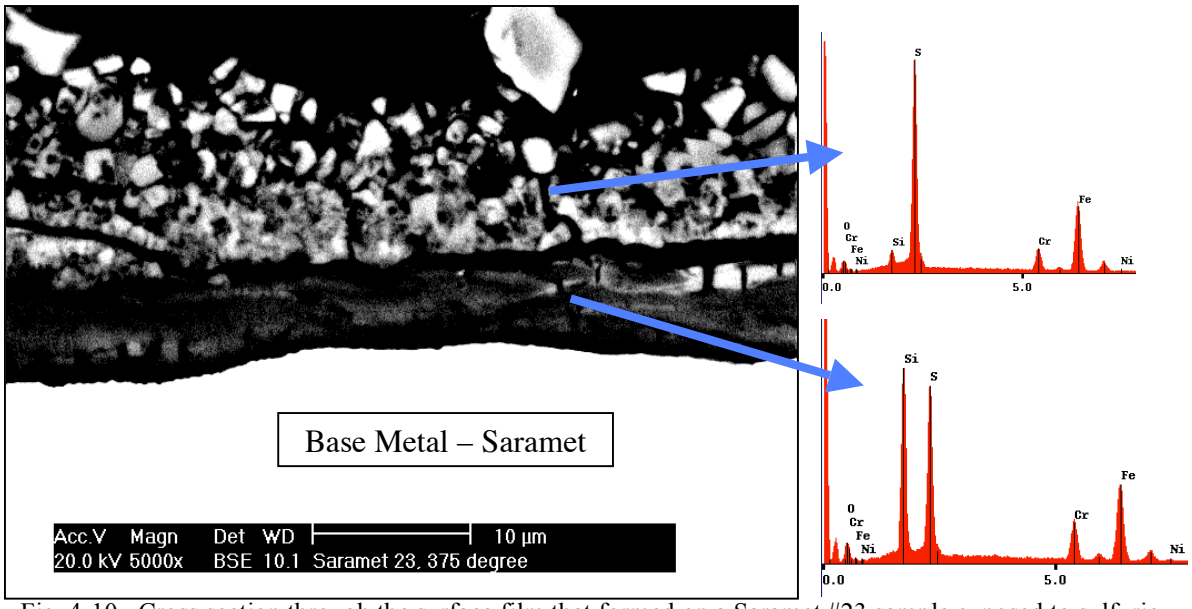

Fig. 4-10. Cross section through the surface film that formed on a Saramet #23 sample exposed to sulfuric acid at 375°C. Composition analysis revealed that the surface laser as Si-rich. (Plot courtesy of T. Lillo, Idaho National Lab.)

Another approach to this problem is to employ ceramic materials. SiC based materials are preferred candidates as both excellent corrosion resistance and high thermal conductivity. Researchers at JAERI have been exploring the use of ceramics materials in boiling H_2SO_4 [M5]. They have shown Si based ceramics such as SiC, Si-SiC and Si_3N_4 to have extremely good corrosion resistance in concentrated H_2SO_4 acid at high temperature and are even better than high Si steel (Table 4-9).

Table 4-9. Corrosion Rate of Si Based Ceramics and High Si Steel in Conc. H_2SO_4 at High Temperature

	H_2SO_4 Acid Conc. and Temp.			
	95 wt% (460°C)		85 wt% (380°C)	75 wt% (320°C)
	100 h	1000 h	100 h	100 h
SiC	-0.1	-0.002	0	0
Si-SiC	0	-0.006	NA	0
Si_3N_4	0	-0.007	0	0
Fe-20Si	1.1	0.13	NA	NA
Fe-Si (annealed)	-0.12	0.065	0	0
Ni-Cr-Si Steel	-0.28	0.96	NA	5 (17 h)

- Original corrosion rate (g/m^2h) from the reference is used.
- -ve value indicates weight gain.

Construction materials capable of handling H_2SO_4 vapor were studied extensively during the early stages of the S-I cycle development as it was thought to be the most critical materials issue of the cycle. Because of the high operating temperature involved, materials candidates were chosen from those that derive their strength from solid solution strengthening instead of precipitation hardening as overage condition can lead to a decrease in strength. Different researchers have come to a similar conclusion that steel with a high Ni-Cr content is most suitable for the decomposition reaction, especially when the operation temperature is above 850°C. At this temperature, it was found that corrosion due to H_2SO_4 vapor is similar to that in air [M18] and thus many qualified high temperature engineering alloys can be suitable. Alloys that have been tested in this environment includes, Incoloy 800H, AISI310, Inconel 600, stainless 304 and a 70Fe-10Ni-18Cr alloy, etc. [M1,M15-M20]. The high Cr content in all these alloys helps to passivate the metal surface. Among all the different candidates, Incoloy 800H has shown the best performance with a corrosion rate of less than 100 μm/yr after a 9000 hr test at 900°C. AISI310 was judged to be applicable to lower temperature application [M16].

Construction materials for vaporization and decomposition of H_2SO_4 have largely been defined by the solar decomposition demonstration that was carried out at Georgia Institute of Technology in 1985 [M2]. A schematic of the solar decomposition experimental set up is shown in Figure 4-11. In this work, concentrated ambient H_2SO_4 (98 wt%) is fed into a dry wall boiler constructed from Hastelloy C-276 operating at around 600°C. Inside the boiler are heated Denstone ceramic balls ($56SiO_2$,-$38Al_2O_3$ wt%). The cold H_2SO_4 acid is vaporized to about 400°C upon contact with these balls. The H_2SO_4 vapor is heated to above 600°C as it passes through a superheater made also with Hastelloy C-276. At this stage, the vapor begins to decompose into H_2O and SO_3. This gas mixture is sent to a decomposer operating at temperatures above 800°C in order for the $SO_3 \rightarrow SO_2 + O_2$ catalytic decomposition to take place. This decomposer was actually a heat exchanger constructed from Incoloy 800H tubes filled with Fe_2O_3 catalyst pallets. Thermal radiation and air heated by the solar tower circulates outside the tubes and manifolds to provide heat for the decomposition reaction. Some of the tubes had an aluminized coating on their inner wall to test the corrosion resistance of such coating. Downstream the un-reacted acid was then condensed in an Incoloy 825 coiled tube and collected. Table 4-10 is a summary of the corrosion performance of the various construction materials tested in the experiment. The oxidation of the high temperature tubing by SO_2, SO_3 and O_2 was found to be the dominant corrosion mechanism and the degree of corrosion is similar to exposure to air. The performance of the selected alloys was satisfactory but oxidation and evidence of corrosion were observed. Moderate corrosion was experienced by all the components and it will need to be reduced in order to assure the long term viable of components.

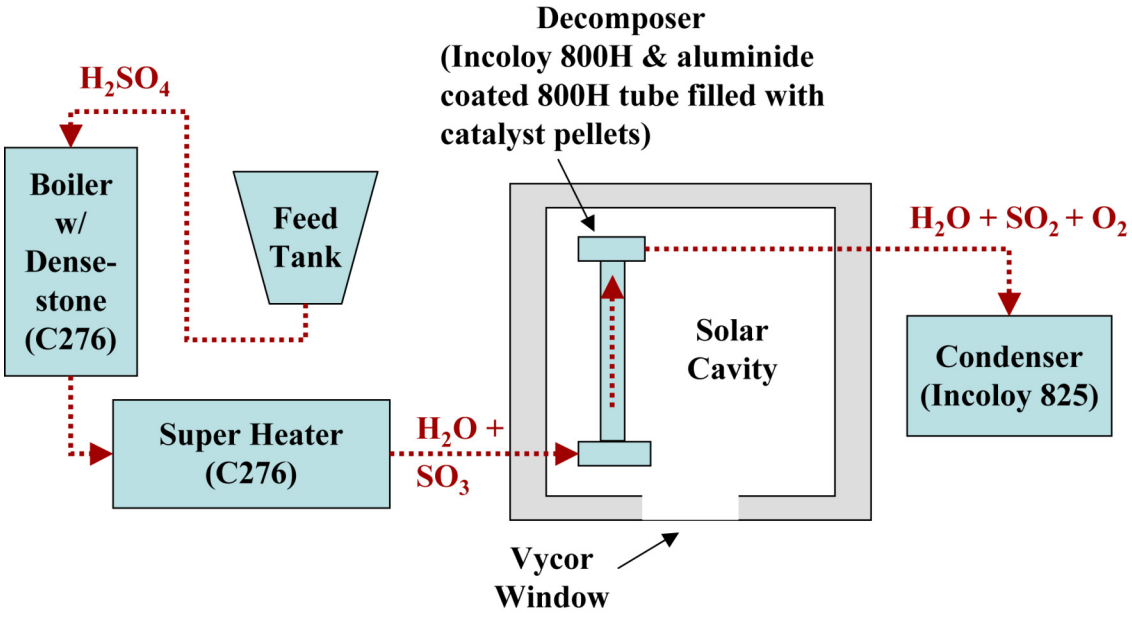

Fig. 4-11. Schematic of the experimental set up for the Solar-H_2SO_4 decomposition experiment.

Table 4-10. Principal Materials of Construction for the H_2SO_4 Solar Decomposition Experiment

Component	Materials	Service Temp. and Media (°C)	Estimated Depth of Corrosion (mil)
Boiler	Hastelloy C-276	>330 (liquid, vapor)	10
Superheater	Hastelloy C-276	600 (vapor)	10
Decomposer tube	Incoloy 800H	850 (vapor)	10
Condenser	Incoloy 825	100-400 (liquid, vapor)	40

The long term corrosion performance and creep characteristics of the alloys in the present environment will need to be addressed in the H_2SO_4 decomposition environment. One must also guard against carbide sensitization, stress corrosion and intergranular crack formation when these alloys are heated for an excessive period of time at high temperature. This is in addition to possible sulfidation of the alloy surface at moderate temperatures due to incomplete chemical reaction where SO_3/SO_2 ratio favor sulfide formation. Only limited long term testing has been carried out and the initial signs have been positive as no stress corrosion cracking has been observed in Incoloy 800H, Inconel 600 and Hastelloy XR tested at 850°C [M9]. Testing is currently under way to study crack formation and growth and creep properties in Alloy 800H, Hastelloy C-276 and other high temperature alloys including Inconel 617 in the H_2SO_4 decomposition environment [M20]. This hopefully will provide insight not only on the high temperature mechanical behavior of these alloys but also the effect of a sulfidizing environment.

In addition to engineering alloys, effort is also on going to develop a SiC based heat exchanger for this application. SiC is extremely stable in this high temperature oxidation environment. The challenge in using these ceramic materials is the processing and joining of materials to accommodate the brittle nature of ceramics. Effort is on going to develop a microchannel plate heat exchanger and the success hinges on the ability to join these plates together. Figure 4-12 shows a prototype of such a microchannel plate that is manufactured from C-SiC composite infiltrated with liquid Si at high temperature. Such manufacturing technique is capable of producing complex profile. It is expected that a heat exchanger constructed from a stack of such plates will be a viable option in the future.

Recently, researchers at Sandia National Laboratory have developed a new H_2SO_4 decomposer design with which the vaporization and decomposition of the acid can be carried with a single bayonet SiC boiler-reactor. Figure 4-13(a) shows a schematic of this design. It consists of an outer SiC feed tube with an SiC outlet tube. H_2SO_4 is vaporized within the outer tube and is then pushed through the catalyst bed for the decomposition

reaction to take place. The decomposed products are channeled out of the reactor through the inner SiC tube and its heat is recuperated in the lower section of the heat exchanger. This design is very efficient but the manufacturing and joining of the various SiC parts remains an obstacle that needs to be overcome.

Fig. 4-12. Prototype of a C-SiC microchannel plate. (Photo courtesy of P. Petersen, UC Berkeley.)

Since the final design and operation conditions of the nuclear S-I hydrogen loop is still being finalized, materials of construction development for H_2SO_4 decomposition will need to proceed with a broad scope. This ensures materials applicable to the final specification will be in place when needed. Table 4-11 lists the various construction material candidates applicable to the sulfuric acid decomposition process. The candidates can be classified into four different categories, superalloys, ceramics, noble metals and intermetallics. Selection will depend on the chemical environment and the manufacturing technique. Even though the surveyed materials have shown good corrosion resistance in H_2SO_4, the effect of chemical contaminants such as traces of HI and I_2 and corrosion species on their corrosion performance is not known. These factors will need to be considered in the development testing process.

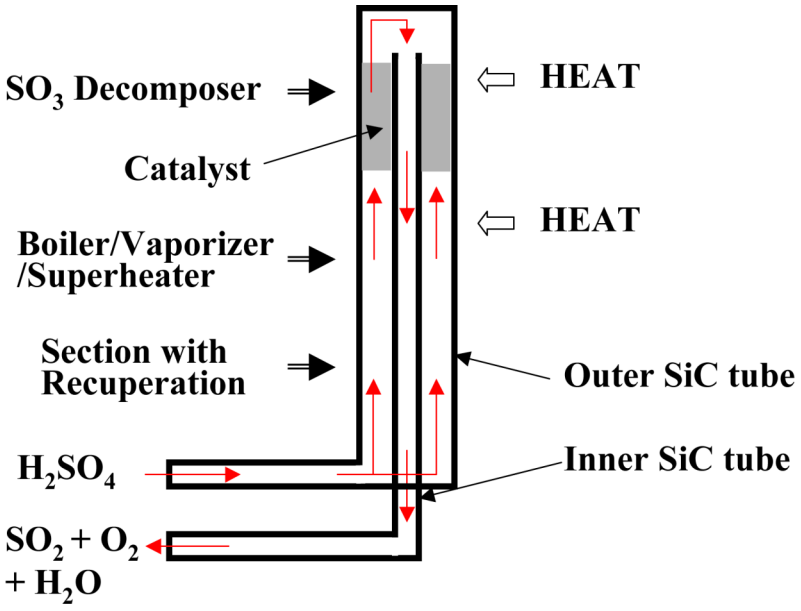

(b)

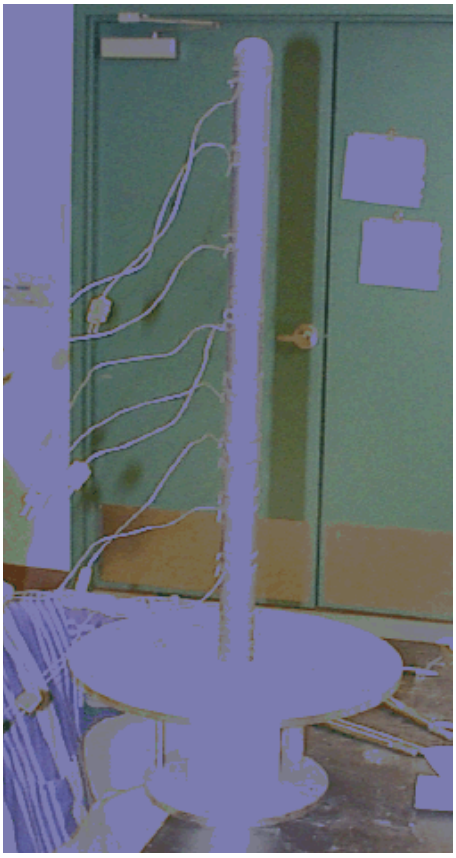

Fig. 4-13. (a) A schematic and (b) a prototype of a SiC bayonet H_2SO_4 vaporizer/decomposer. (Photo courtesy of F. Gelbard, Sandia National Lab.)

Table 4-11. Summary of Materials Options for the Sulfuric Acid Decomposition Process

Process Regime	Conditions	Candidate Materials	Compatibility	Comments
H_2SO_4 concentration	25°–180°C, 50 wt% 25°–150°C, 50-75 wt% 180°–450°C, 75-95 wt% H_2SO_4, iodine species, impurities	Glass lined steel, plastics, ceramics Hastelloy B-2, C-276 Incoloy 800H, AL610, high Si steel, Au or Pt plating/cladding	Hastelloy B-2 < 0.1 mm/yr for concentrations up to 60% High Si steel corrosion ~0.1 mm/yr for concentrated acid, higher for low concentrations	Concentration may require multiple materials Options identified for all concentrations and temperatures Evaluate coatings, plating and cladding B-2 promising at low concentration High Si steel fabrication issues
H_2SO_4 vaporization	350°–550°C, H_2O+SO_3, iodine, other contaminants	Structural: Incoloy 800H AL610, high Si steel SiC, Si_3N_4 Hastelloy G, C-276	800 H, 800 HT High Si steel (SiO_2) <5 mpy SiC ~ no corrosion in 1000 h test at 75%–95% acid (JPN) C-276 ~1 mm/yr at 476 h	Coated materials (Pt) cost issue Ceramics promising, but have fabrication and joining issues Dry wall boiler design with ceramics may be option Data needed with iodine contamination
H_2SO_4 decomposition	550°–950°C, H_2O, H_2SO_4, SO_3, SO_2, O_2	Structural: Incoloy 800 HT, Incoloy 800 H (with aluminide coatings), AL 610 Ceramics, Pt or Au coatings on superalloy structural materials	Incoloy, inconel bare – 2–4 mg/cm^2 in 1000 h at 900ʃC Aluminide coatings – approx. 1 mg/cm^2 in 1000 h at 900°C Intergranular corrosion observed for 800 H Noble metal coatings may provide corrosion protection	Incoloy 800 HT may address intergranular corrosion C-SiC composites should be examined Pt coating may serve function of catalyst and reduce corrosion Corrosion benefits of noble metal coatings must be demonstrated

4.11. MATERIALS OF CONSTRUCTION FOR SECTION III

As discussed in Sections 4.3 through 4.6, there are two pathways to carry out HI decomposition and the respective process steps are listed in Tables 4-3 and 4-4. Construction materials development has focused on identifying materials that can withstand the different acids and chemicals at the processing conditions. HI_x acid and vapor are present in both distillation processes whereas H_3PO_4 is only used in extractive distillation. Hence, the following discussion of candidate construction materials for Section III will be based on chemical contents instead of processing environment as was the case for the other two sections. First, data for general corrosion will be reviewed followed by the effects of stress corrosion and chemical contamination.

4.11.1. Materials for HI_x

Corrosion data of materials in HI_x is extremely limited. The most comprehensive set is from Trester, *et al.* [M1]. Table 4-12 lists a summary of the immersion coupon test results from their work. The test temperature is similar to that for extractive distillation and is about 100°-200°C lower than that required by reactive distillation. Based on this data, Ta, Nb, Mo (refractory metals), Zr (reactive metals), SiC (ceramics) and carbon based materials have the best prospect of being compatible with HI_x at higher temperature.

Immersion coupon tests have been conducted at General Atomics to study the corrosion resistance of a variety of construction material candidates in HI_x at temperatures used for extractive distillation [M19]. Figure 4-14 shows the progression of an immersion coupon test of a Ta-2.5W coupon in HI_x at 310°C for 2000 h. No evidence of corrosion, including the weld region, can be observed. This can be compared with a Zr_70_5 coupon that shows extensive dissolution after only 120 h in the same environment (Figure 4-15). Immersion coupon testing has shown that Ta and Nb alloys have the best general corrosion characteristics among the different metals when tested against HI_x at high temperatures (Table 4-13). Tests are on going to understand the effect of an HI_X environment for occurrence of nucleation and the growth of cracks in Ta and Nb alloys that showed good corrosion properties.

SiC based materials have also shown very good corrosion resistance in HI_x. Both sintered and CVD SiC have very low corrosion rate when tested in HI_x at elevated temperatures. In addition, Si infiltrated C-based materials (Si-SiC) also have good potential. This method of manufacturing may become an attractive option in the future as

Table 4-12. GA Results (1977-1981) Summary from Trester and Staley [4]

Test	HI (%)	I_2 (%)	H_2O (%)	Temp (°C)	Ti Pres.	me (h)	Materials Tested		
							Excellent	Fair	Poor
1	20[1] (4)[2]	20 (2)	60 (93)	25	Atm	8760	Mo, Nb-1%Zr, Ta, Ta-10%W, Ti(as cast), Ti-0.5%Pd, Zr, Zircaloy2 TFE, FEP, Kalrez 1050, Kel-F 3700, Fluorel 2174, Viton A, Parker V-834-70	Chlorimet 2 and 3, Hastelloy B2 and C276 PVC, polycarbonate, Vespel Sp.1, CPE, FETFE	Inconel 600, Monel, Haynes, Hastelloy G, 304 stainless Nylon, mylar, silicone
2	30 (15)	50 (13)	20 (72)	300-500	13.1–17.2 MPa	5–10	Mo, Ta	Ti Inc	onel 600
3	11 (11)	82 (40)	7 (49)	100	Atm	3170	Mo, Nb-1%Zr, Ta, Zr TFE, FEP, PFA, tefzel (teflon) SiC, alumina, boronsilicate glass	Ti–0.2%Pd(annodized), Hastelloy B2, Durichlor 51, Zircaloy2, Zr702 Kynar 450 Zirconia	Duriron D, Chlorimet 2, Hastelloy B2 and C276, Ti-0.5%Pd, gold, platinum CPVC, polypropylene
4	11 (11)	82 (40)	7 (49)	120	Atm	500	Mo, Nb, Nb-1%Zr, Ta Alumina, vitreous carbon	TFE, FEP, PFA	Lead Viton VTX 5362, Viton B, carbonrundum
5[3]	24 (12)	55 (14)	21 (74)	135	Atm	178	Mo, Nb, Nb-1%Zr, Ta, Zircaloy2, Ta-10%W, Zr	Ti–0.5%Pd T	Ti-0.2%Fe-0.25%O (anodized Ti)

[1]wt%, [2]molar%, [3]Circulating HI_x.

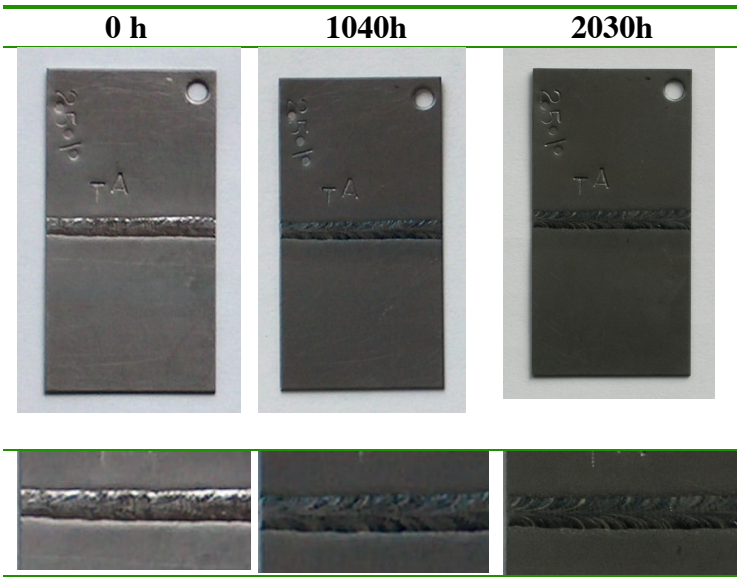

Fig. 4-14. A Ta-2.5W coupon with an e-beam weld that has been immersion tested in HI_x at 310°C.

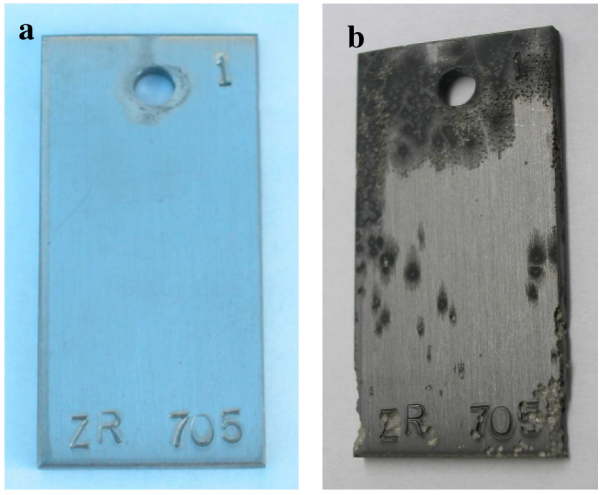

Fig. 4-15. Zr_70_5 coupon (a) before and (b) after a 120 h test in HI_x at at 310°C.

they promise an extremely low cost alternative to manufacture SiC-based corrosion resistant materials [M17] and reduce the potential joining problems. Effort is continuing to resolve the manufacturing techniques and improve the inherent mechanical properties of these SiC based materials.

Other ceramic materials such as Al_2O_3 or mullite have also been shown to be stable in the presence of I_2 and HI_x but their application in traditional heat exchanger design is

limited as they have very low thermal conductivity even relative to SiC. On the other hand, recent modeling results from micro-channel heat exchanger indicated that there may be an advantage in using low thermal conductivity material in these designs. Even though there are still many obstacles to using them in the near future, ceramic-based components will most likely play an important role as the S-I cycle develops.

Table 4-13. Corrosion Rate of Various Materials in HI_x at High Temperatures

	Corrosion Rate (mils/yr)	
Material	**Boiler (310°C)**	**Feed (262°C)**
Nb-7.5Ta	-3.90	0.39
Splint Si-SiC	-3.31	0.00
SiC (sintered)	-2.60	0.00
Ceramatec SiC (sintered)	-1.06	0.00
Mo-47Re	-0.67	0.00
SiC (CVD)	-0.55	-0.55
Ta	-0.51	0.08
Ta-2.5W -2	0.00	0.00
Ta-2.5W -1	0.04	0.00
Ta-10W	0.04	-0.24
Nb-10Hf	0.04	0.00
Ta-40Nb	0.28	-0.08
Nb	0.43	0.00

- Weight loss; + Weight gain.

4.11.2. Materials for Phosphoric Acid

Phosphoric acid is a chemical reagent commonly used in the chemical industry. However, most of the corrosion data of materials in H_3PO_4 is for acid concentration up to 85 wt% whereas the H_3PO_4 concentration in Section III ranges from 85–96 wt%. High Mo stainless steel such as Alloy 28 and G-30 are commonly employed in the chemical industry to contain H_3PO_4. In addition, Ni-Mo alloys are also widely used. Table 4-14 lists the corrosion rate of a number of metals in 85wt% H_3PO_4 [M14]. At high acid concentration and at the boiling temperature of 158°C, it has been shown that Ta, Nb and their alloys have good corrosion resistance in the acid and are good candidates for materials of construction. Table 4-15 shows the corrosion rate of Ta and Nb alloys in 80% conc. H_3PO_4 at 150°C and 200°C respectively [M16].

Table 4-14. Corrosion Rate of Alloys in H_3PO_4

Alloy	Concentration	Temperature (°C)	Corrosion Rate (mils/yr)
316 stainless	85	115	5.91
Hastelloy C	85	Boiling	44.90
Durimet 20	75-85	115	9.06
Haynes 556	85	Boiling	33.08
Inconel 617	85	Boiling	25.99
Monel 400	85	124	10.24
Tantalum	85	100	0.00
Niobium	85	100	5.12
Silver	85	140	1.97

Table 4-15. Corrosion Rate of Ta and Nb Alloys in 80% Conc. H_3PO_4 at 150°C and 200°C

	Corrosion Rate (mils/yr)	
Alloy	150°C	200°C
Niobium	59.06	NA
Nb-20Ta	11.81	NA
Nb-40Ta	8.66	492.13
Nb-60Ta	2.76	82.68
Nb-80Ta	0.39	29.92
Tantalum	0.05	5.31

Since both HI and H_3PO_4 are reducing in nature, it is possible to use materials that are common to both in the iodine separation reaction (Table 4-3). The material of construction used to fabricate the I_2 separation reactor must to able to resist the combination of HI_x and H_3PO_4. Preliminary test results show that the corrosion behavior of the various materials test in the HI_x - H_3PO_4 acid mixture is similar to those in HI_x at high temperatures with Ta and Nb alloys and SiC based materials as the most promising construction materials candidates.

4.11.3. Materials for HI + H_3PO_4 and Iodine (Iodine Separation)

Construction materials used for the iodine separation step in Section III will encounter a flowing mixture of HI_x and H_3PO_4, a light HI + H_3PO_4 upper phase and a

denser iodine rich lower phase that forms in the separator (Section 4.6.1). Materials candidates for use in HI_x and H_3PO_4 have been discussed previously. However, mixing of various acids may lead to synergistic corrosion effect. Figure 4-16 shows a Nb-10Hf coupon that has been tested in a static HI_x and H_3PO_4 mixture that represents that iodine separator environment. A scale has formed on the coupon where it is in contact with the H_3PO_4 rich upper phase. This can be compared with a Ta-10W coupon tested in the same environment (Figure 4-17). Table 4-16 shows a summary of the corrosion rate of various materials that have been tested in the HI + H_3PO_4 and the results show that Ta and its alloys and SiC based materials are suitable for this environment.

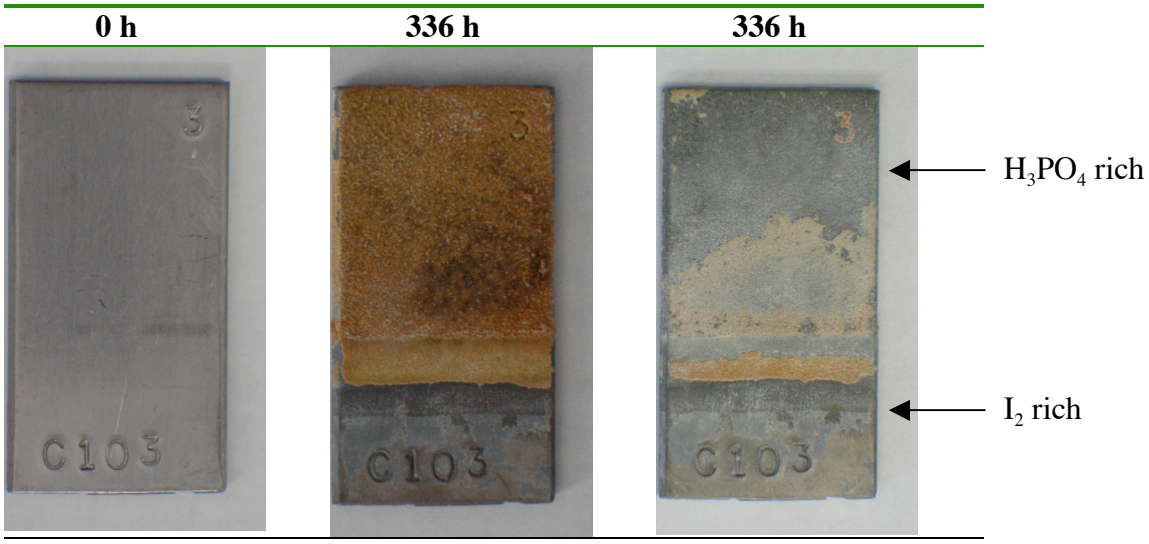

Fig. 4-16. A Nb-10Hf coupon tested in a static HI_x-H_3PO_4 mixture at 140°C for 336 h (a) new, (b) post test and (c) post test with scale removed.

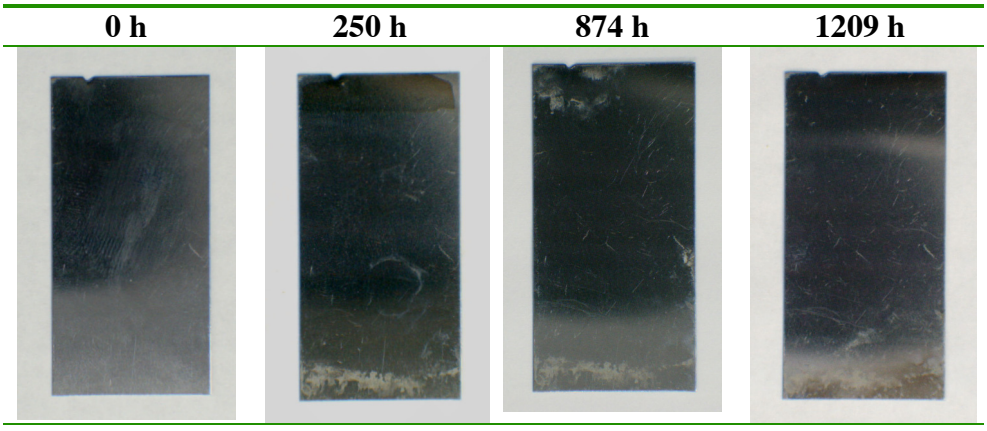

Fig. 4-17. A Ta-10W coupon tested in HI_x-H_3PO_4 at 140°C for 1209 h.

Table 4-16. Corrosion Rate of Various Materials Tested in a HI_x-H_3PO_4 Mixture at 140°C for 120–1100 h

Alloy	Corrosion Rate (mils/yr)
Ta-10W	0.02
Ta-2.5W	0.03
SiC	0.08
Ta	0.11
Mo	0.45
Nb-1Zr	24.88
Nb	38.96
Nb-10Hf	40.55
Zr 705	91.44
Hastelloy B2	137.35
C-276	140.08
C-22	147.28
Nb-7.5Ta	187.10
Monel	225.77

Based on data obtained so far, it appears that liquid processes in Section III will rely heavily on Ta and Nb alloys as construction materials. Since these metals are expensive in nature and have low yield strength, one must explore different manufacturing means to reduce the overall component cost and enhance the mechanical properties of components. For example, cladding can be used to bond a Ta layer to a base material to take advantage of it corrosion characteristics while keeping the cost down. Techniques for cladding or lining are well established and suitable means will need to be selected for the application. Figure 4-18 shows a Ta plated stainless washer that has been tested in a HI_x and H_3PO_4 acid mixture. Its corrosion performance is similar to that of Ta alloys in the same environment (Figure 4-18). Other surface coating or modification techniques such as PVD processes and ion-implantation may help to fabricate components in addition to cladding, lining or plating. The application of such materials processing technology to manufacture process components will need to be explored.

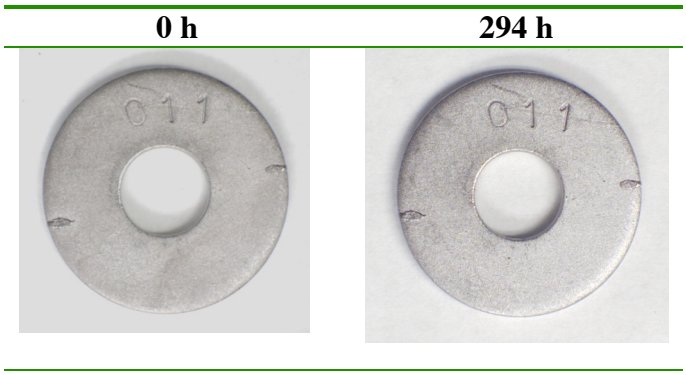

Fig. 4-18. A stainless washer that has been plated with a Ta layer and tested in HI_x-H_3PO_4 acid mixture at 140°C for 294 h.

4.11.4. Materials for HI + I_2 + H_2 (Gaseous HI Decomposition)

In extractive distillation, the HI → H_2 + I_2 decomposition reaction is carried out in the gas phase between 300°-450°C (Table 4-3). Given that both HI and I_2 will be in gaseous form, the corrosiveness of the environment is reduced. Since refractory Ta and Nb alloys exhibit internal oxidation at of 350°C and above, their application in this environment will be limited. Onuki, *et al*. had screened a number of engineering alloys and corrosion resistant materials in a HI/I_2/6H_2O gaseous environment at temperatures between 200°– 400°C [M6]. Metallic Ta, Zr, Ti and SiC and SiN show very low corrosion rates at all temperatures. Based on the screening results, they conducted 1000 hours long term testing on selected materials and their results is shown in Table 4-17. Scale formation and discoloring were observed in all specimens. They suggested that high temperature oxidation of the metal surfaces leads to a protective scale which limits the corrosion of metals in this environment. The H_2O fraction in their test environment is much higher than that stated in the flowsheet. Hence, the applicability of the engineering alloys will need to be verified. Trester et al. also conducted preliminary testing of Hastelloy B and C-276 in an HI + I_2 environment in the absence of moisture. They concluded that both alloys can be used in this environment [M1]. Unlike reactions involving liquid phases, it appears that commonly available corrosion resistant engineering alloys can be used for the HI gaseous decomposition process but this will require more long term testing to confirm. Table 4-18 summarizes a compatibility chart of construction materials that are applicable to the different processes in Section III.

4.11.5. Effect of Stress Corrosion and Chemical Contaminants

In terms of general corrosion, one or more preliminary construction material candidate for each of the S-I cycle processing steps have been identified. However, materials are subjected to processing and environment effects which could lead to

susceptibility to stress corrosion phenomenon. Fabrication methods such as welding, machining and hot and cold forming can modify the corrosion resistance of materials that may have shown good general corrosion characteristics. Investigative work has been on going to study such environmentally-assisted crack initiation and growth phenomena in C-ring, U-bend, double cantilever bean (DCB) and compact tension (CT) specimens in both liquid and gaseous test environment at General Atomics. Figure 4-19 shows a Zr_70_5 C-ring specimen that was immersed in HI_x at 310°C for 120 h; a crack was observed after testing. This can be compared to a Hastelloy C22 U-bend specimen that has been tested in the HI gaseous decomposition environment at 450°C for 1570 h, in which no crack was observed (Figure 4-20). Since Section III will be operated in a pressurized environment, stress corrosion properties of candidate materials will need to be considered.

Table 4-17. Corrosion Test Results in a Vapor Medium of HI–I_2–H_2O (1/1/6) Vapor at Various Temperatures for a 1000 h Duration

	200°C			300°C			400°C		
	I	II	III	I	II	III	I	II	III
Fe-1Cr-0.5Mo	BK	R	3.94	DB	R	3.94	BK	R	7.88
SUS444	BK	P	3.94	DB	R	7.88	GB	R	7.88
SUS315L	BK	N	3.94	DB	R	7.88	BR	R	7.88
Inconel 600	BK	N	0	DB	N	0.05	BK	R	3.94
Hastelloy C-276	BK	N	0	DB	N	0	BK	R	1.87
Ti	N	N	0	N	N	0	GR	N	0

I Surface appearance. N = no scale, BK= black, DB = dark brown. GB = greenish brown, BR = brown, GR = gray.
II Surface appearance after descaling. N = no change, P = pitted, R = roughened.
III Corrosion rate in mils/yr.

Another key issue that needs to be addressed during materials development is the effect of contaminants within the process streams. There are a number of liquid-liquid separation steps within the S-I cycle that result in a trace amount of chemical contamination in the separated liquid stream. The presence of such contaminants may affect the corrosion performance of materials. Table 4-19 summarizes the contaminants that can exist in the different process fluids. The only previous experiment that addressed this involves the effect of a minor amount of HI in the H_2SO_4 of Section I (Table 4-7). More recent investigations on this subject at General Atomics have illustrated the

potential pit falls of contamination. Figure 4-21 shows the effect of contaminants on the corrosion performance of C706 (Cu-Ni alloy) in concentrated phosphoric acid. Even though C706 exhibits satisfactory corrosion rate in 96 wt% H_3PO_4 and the acid with a trace amount of HI, it corrodes rapidly when a trace amount of I_2 is added into the acid complex. This shows that much more work remains to be done to understand contamination effects.

Table 4-18. Materials Options for Section 3: Hydrogen Iodide Decomposition

Process Regime	Conditions	Candidate Materials	Compatibility	Comments
Reactive distillation - reactor HI_x feed ($HI + I_2 + H_2O$)	250ºC, ~40 bar Impurities, H_2S, S, etc.	Ta and alloys, Nb and alloys, Mo SiC	Pure Mo and Ta <0.1 mm/yr Hydrogen embrittlement effects	Processing effects unknown Evaluate coatings, plantings Fabrication and cost issues
Reactive distillation -reactor bottom HI_x with high I_2 concentration (<85%)	310ºC, ~40 bar Sulfur species contaminants	Ta and alloys, Nb and alloys, SiC, Si-SiC, mullite	W, Mo and Ta <0.01 mm/yr in pure iodine at 300ºC Gold and Pt works well in pure iodine but performs poorly in HI_x	SiC composites should be examined Materials need to be compatible with the HIx feed for reactor application
Extractive distillation – Iodine separation HI_x and concentrated H_3PO_4	120ºC, atm press Contaminants from other sections – H_2SO_4	Ta and alloys SiC and carbon composite	Ti and Hastelloy B2 compatible with HI_x below 150ºC	Carbon composite can be consider for lower temperatures
Extractive distillation – Phosphoric acid concentration	250ºC, atm press Contaminants from other sections – HI_x, H_2SO_4	Ta and alloys SiC and carbon composite		Systems level design considerations in the integration of different materials
Extractive distillation – HI gaseous decomposition	300º-450ºC, atm press Contaminants from other sections – H_2SO_4	Hastelloy B and C-276, Ti SiC and carbon composite		

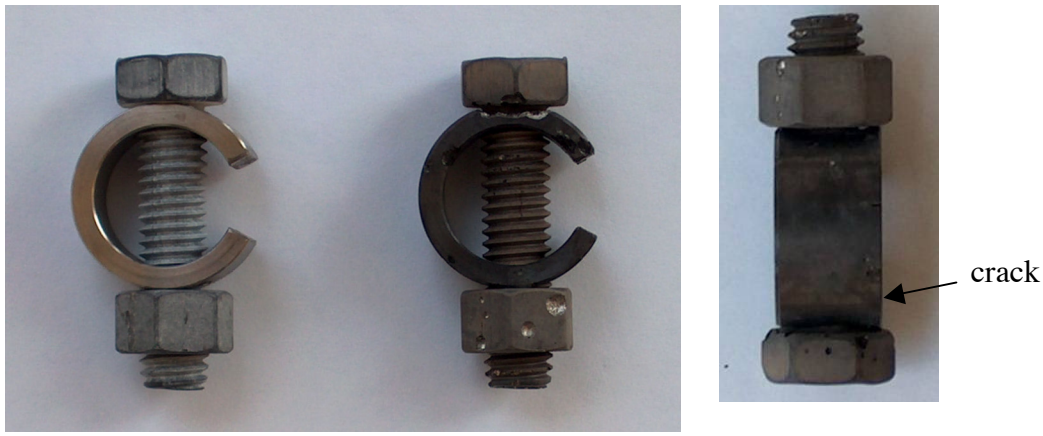

Fig. 4-19. A Zr_70_5 C-ring specimen under tensile loading to 98% of yield stress that has been tested in HI_x acid. Cracks and pit developed in the C-ring specimen after test.

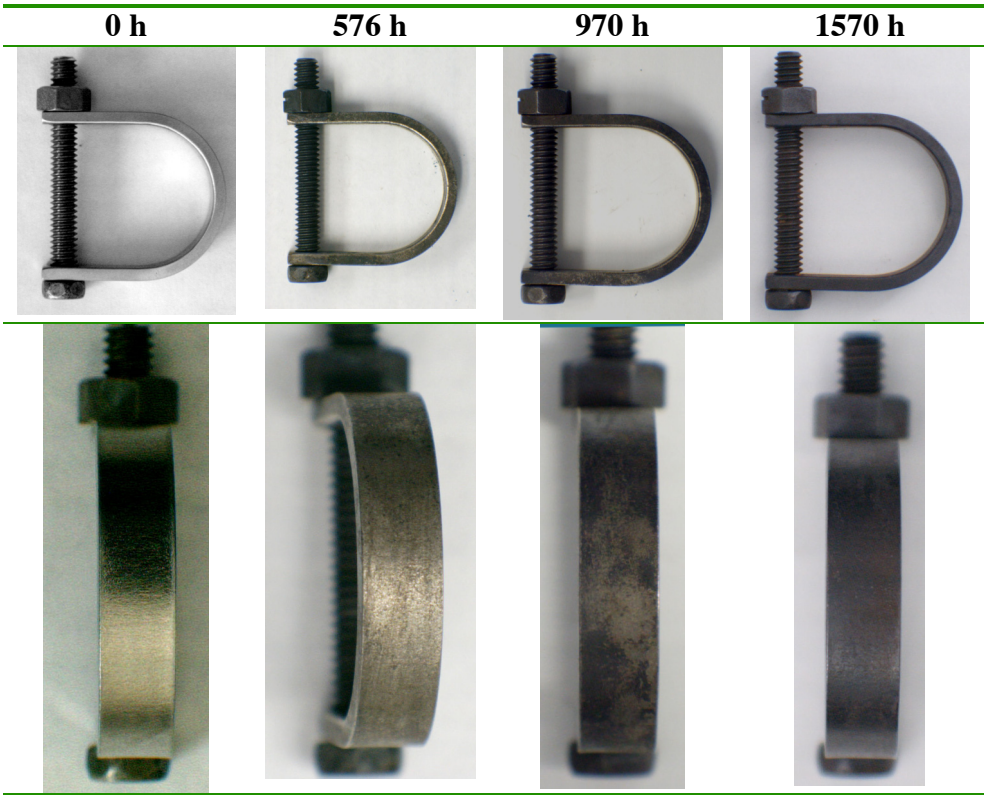

Fig. 4-20. C22 U bend specimen coupon tested in the gaseous HI gaseous decomposition environment ($HI + I_2 + H_2$) at 450°C.

Table 4-19. Contaminants in Process Streams that May Affect the Corrosion Environment

Section	Process	Contaminants
II	H_2SO_4 concentration	• HI_x from Section I • Corrosion products from other sections
III	Iodine separation	• H_2SO_4 from Section I corrosion products from other sections
III	H_3PO_4 concentration	• H_2SO_4 and HI_x from Section I and iodine separation • Corrosion products from other sections
III	HI distillation (reactive and distractive)	• H_2SO_4 from Section I • Corrosion products from other sections

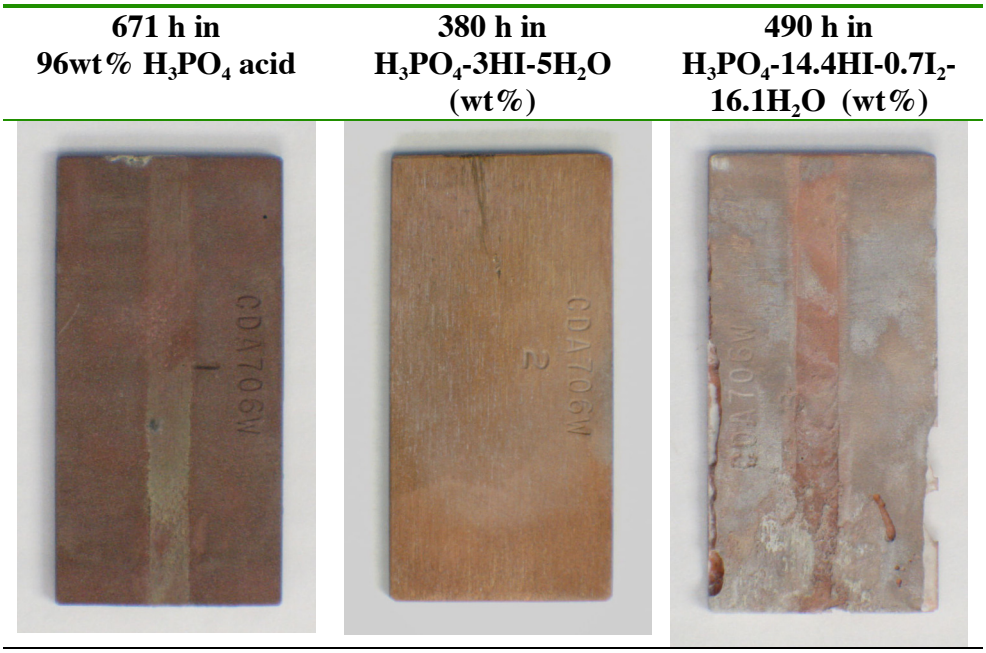

Fig. 4-21. C_70_6 (Cu-Ni) alloy coupons tested in (a) conc. H_3PO_4 acid, (b) conc. H_3PO_4 acid with a trace amount of HI and (c) conc. H_3PO_4 acid with a trace amount of HI and I_2. The addition of trace amount of I_2 leads to a dramatic increase in corrosion of C_70_6 in H_3PO_4.

4.12. SEPARATION MEMBRANES

Separation membranes can be extremely important to the economical success of the S-I cycle as they can improve the overall efficiency of the cycle though removal of water, SO_2 and H_2 from the chemical stream. This can reduce the amount of excess heat needed to boil off the water and improve the conversion efficiency of decomposition reactions. There are three potential membrane applications within the S-I cycle:

1. H_2O separation from the HI_x liquid phase from the Bunsen reaction to reduce the heat input required in the subsequent distillation processes.
2. SO_2 separation from the H_2SO_4 decomposition gas product stream to improve the conversion efficiency and perhaps shift the reaction to a lower temperature.
3. H_2 separation from the HI gaseous decomposition reaction to reduce the amount of recycle.

4.12.1. H_2O Separation

Nafion-117, a perfluorinated polymer membrane, has been studied for use in a direct separation of H_2O from HI_x. Its ability to remove H_2O from a flow stream of HI_x at 125°C has been successfully demonstrated (Figure 4-22). The permeability or flux through the Nafion-117 membrane is temperature dependent and is inversely correlated to the water concentration [T1,T3].

Nafion membranes have also been used to carry out other concentration scheme. Hwang, *et al.* have employed an electro-electrodialysis approach to raise the concentration of HI within the HI_x solution at 110°C [T6]. Nafion acts as a cation exchange membrane in an electrolysis cell in which HI is formed at the cathode. This raises the HI concentration within the HI_x catholyte (Figure 4-23). In addition to this, the increase in HI content helps to break up the azeotropic between HI, I_2 and H_2O and facilitates the distillation of HI from HI_x. Researchers at JAERI have taken this concept a step further and explored the possibility of using Nafion membrane to run a electrochemical membrane Bunsen reactor [T4,T5].

Long-term testing has shown stable transport characteristics in Nafion when operated at the Bunsen reaction temperature, but more testing is needed [T3]. The transport kinetics, permeability and the capability to manufacture membrane of substantial area are key issues that need more research and development. There are ample opportunities to test other membranes for this application.

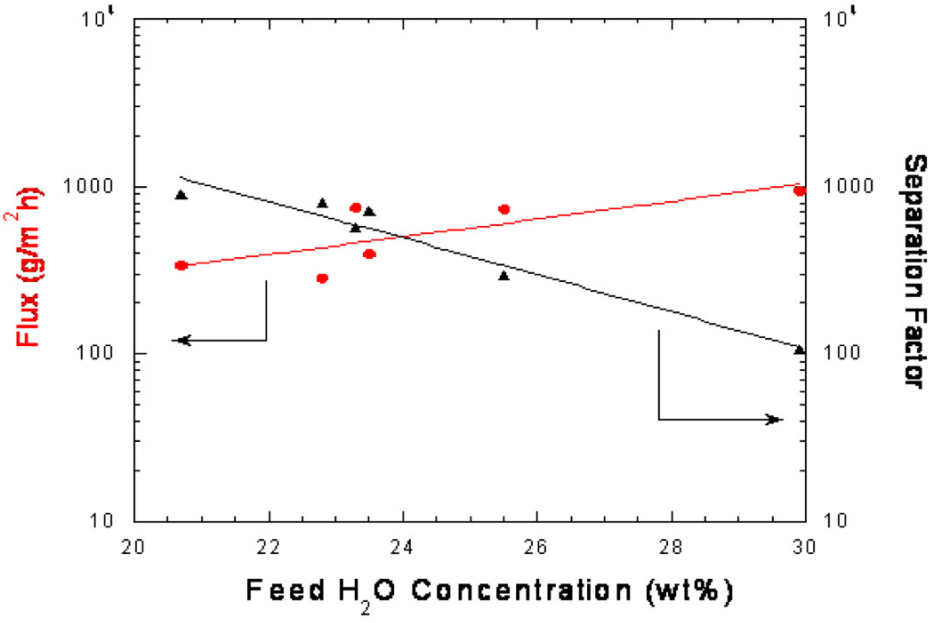

Fig. 4-22. Nafion –117® performance using an HI/Water/I_2 feed at 125°C. (Plot courtesy of F. Stewart, Idaho National Lab.)

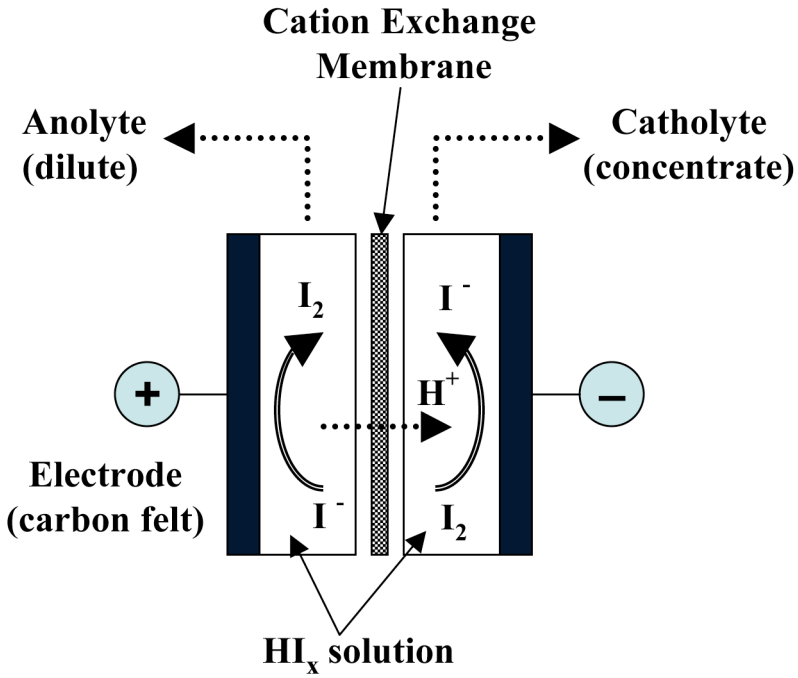

Fig. 4-23. Schematic of the electro-electrodialysis process to concentrate the HI_x acid feed from the Bunsen reaction.

4.12.2. SO_2 Separation

The second possible application of membrane in the S-I cycle is to separate SO_2 from SO_3 and O_2 gases during the $SO_3 \rightarrow O_2 + SO_2$ decomposition reaction. The biggest challenge is that membrane will have to operate at temperature between 800°-950°C and no existing commercial membrane has been shown to meet these requirements. Work is underway at Oakridge National Laboratory to identify and test suitable porous ceramics that are capable of this application.

4.12.3. H_2 Separation

In the gaseous HI decomposition reaction, H_2 separation membranes can play a critical role. The decomposition reaction $HI \rightarrow H_2 + I_2$ is an equilibrium reaction that has a conversion efficiency of around 22% at 450°C. One can enhance the decomposition rate by removing hydrogen from the reactor. Therefore, functional membranes that can separate hydrogen from the reactor will lead to a reduction in the amount of HI gas that needs to be recycled through the reactor. In addition, an effective separation membrane can maintain the purity of the H_2 gas produced. A number of hydrogen separation membranes that have been developed for many applications. Unfortunately, most of them employ metals such as Pd, Pd-Ag and Zr. Since these materials have been shown to be susceptible to corrosion in an iodine rich environment, they are not suitable for this application. Hwang, *et al.* have prepared silica membranes by CVD that have shown high permeability of H_2 from a H_2-H_2O-HI gaseous mixture at elevated temperatures (Figure 4-24). A separation factor of more than 600 between H_2/HI has been observed [T2,T7]. The importance of such separation membrane has been demonstrated by Nomura *et al.* They calculated that the use of such membranes can improve the overall cycle thermal efficiency by 1% [T10]. Ideally, the membrane should have a high thermal conductance so that a membrane reactor can be used [T9]. There is a need for the development of such a membrane possibly using porous SiC or SiC based materials. The manufacturing process of the silica and other membrane will need to be addressed to improve the reliability and cost of such tubular membrane-reactor.

4.13. CATALYSTS

The sulfuric acid and the HI decomposition reactions in Sections II and III are both catalytic processes. A variety of oxides, activated charcoal and platinum have been employed as the catalyst for these reactions. On going research in this area is trying to identify the optimal catalyst support to minimize the overall cost and the integration of the catalyst into the process systems.

a

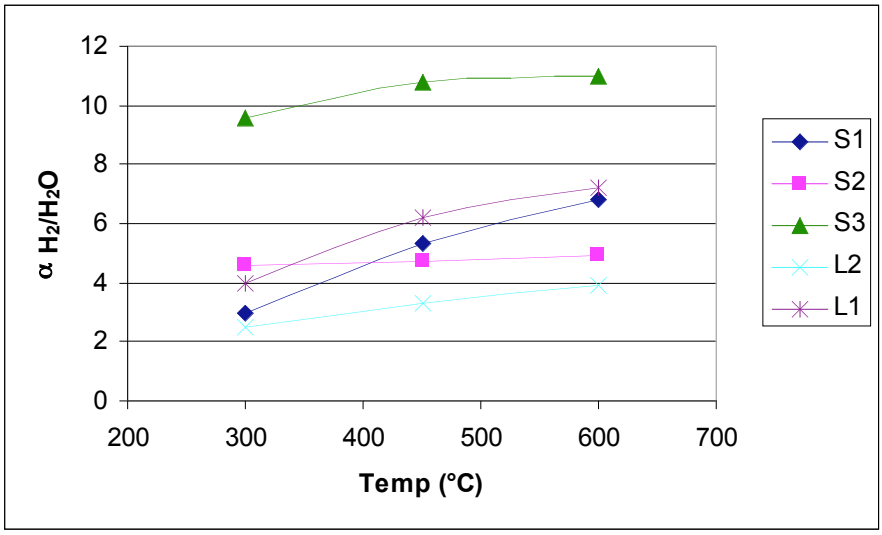

b

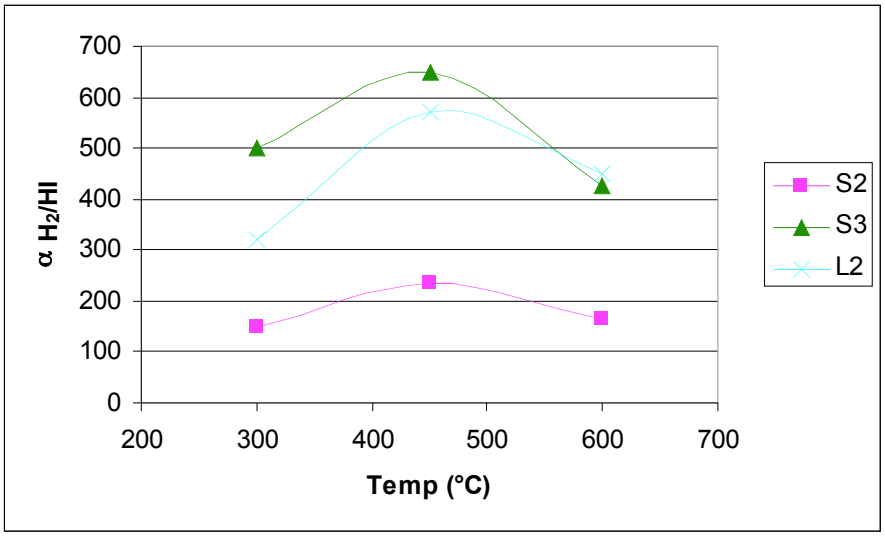

Fig. 4-24. Separation factor of H_2 from H_2-HI-H_2O for various silica membranes.

4.13.1. Sulfuric Acid Decomposition

As mentioned in Sections 4.3 through 4.6, the catalytic decomposition reaction $SO_3(g) \rightarrow SO_2(g) + \frac{1}{2}O_2(g)$ is carried out at 850°C and above in order to obtain appreciable conversion rate. The reaction is greatly enhanced by the application of a catalyst. However, catalysts have been observed to fail due to formation of volatile acid, which causes support poisoning and catalyst attrition at this temperature [C1,C3]. If an optimum catalyst can be identified, the reaction temperature can be lowered.

The first solar demonstration H_2SO_4 decomposition experiment employed Fe_2O_3 pellets as catalyst. They were packed inside the tubes of a heat exchanger. Adequate

decomposition took place but breakdown and minor wear of the pellets were observed. Figure 4-25 shows a plot of SO_3 conversion as a function of temperature for various catalysts [C2]. The carrier gas is N_2 which contains 4 mol% of SO_3 flowing at atmospheric pressure. Based on experimental results, it was found that the order of activities is $Cr_2O_3 > Fe_2O_3 > CuO > CeO_2 > NiO > Al_2O_3$. At temperature higher than 700°C, the activity of Cr_2O_3 is similar to that of platinum at atmospheric pressure. One of the drawbacks in using oxides as a catalyst in this reaction is that they have a tendency to form metal sulfate at lower temperatures which reduces their activity for the reaction. In addition, the vapor pressure of these oxides is not negligible at this high working temperature which may affect their long term performance. Work is on going to identify oxide based catalyst that does not subscribe to sulfate formation. For now, platinum, despite its high cost, is the preferred catalyst for sulfuric decomposition [C1].

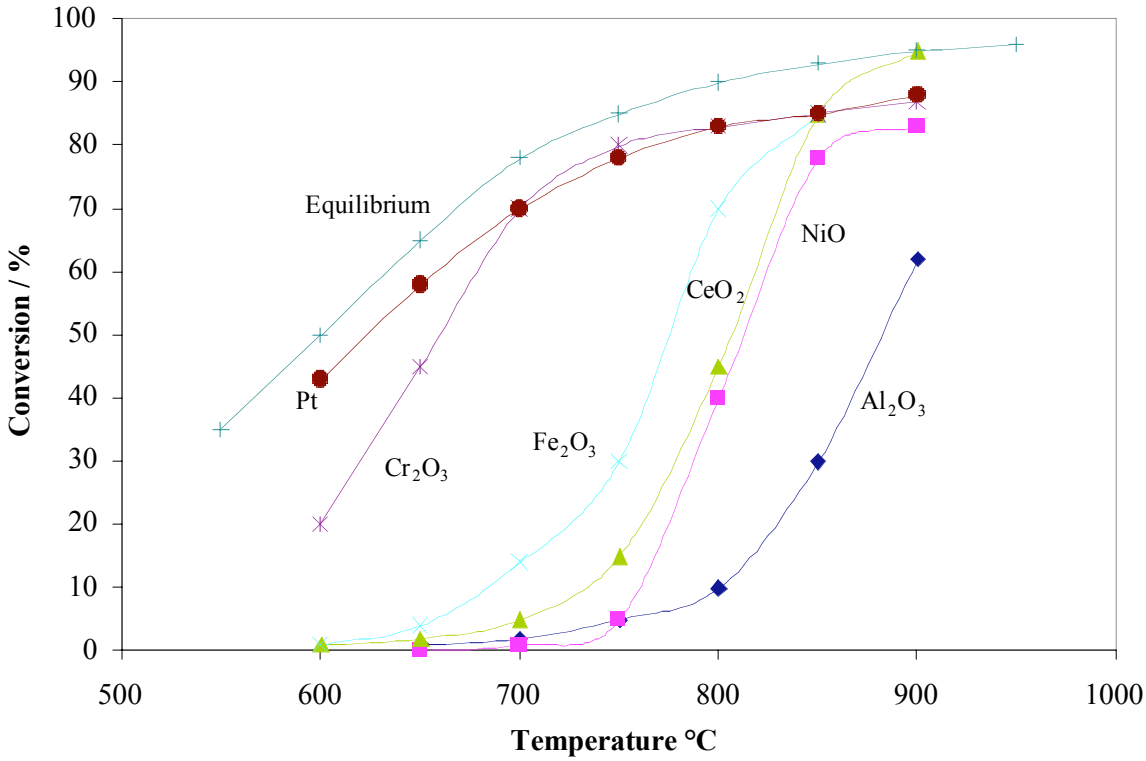

Fig. 4-25. Relationship between conversion to $SO_2 + H_2O$ and temperature for catalytic metal oxides and Pt in a N_2 flow containing 4 mol% SO_3 at a space velocity of 4300 h^{-1}.

The Pt catalyst needs to be supported to reduce cost and this is commonly done by plating Pt onto porous metal oxide such as Al_2O3, TiO_2 and ZrO_2 at about 0.1 wt%. Such catalyst is commercially available. Pt-based catalysts need to have high catalytic activity and stability. They are controlled in turn by factors such as interaction with the reaction environment, support poisoning, the amount of exposed surface area and formation of

acid salts. Of the commercially available catalyst that has been tested, the conversion rate decline as testing continues (Figure 4-26). Working is on going to find a suitable support and loading fraction to assure the long-term performance.

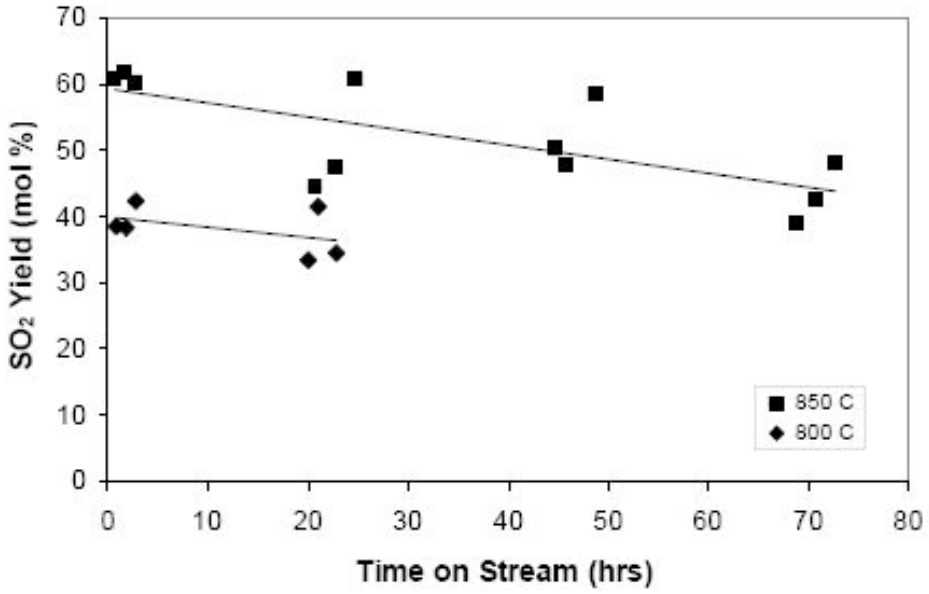

Fig. 4-26. Stability of 1 wt% Pt/ZrO_2 catalyst in stream of $H_2O + SO_3$ ($\rightarrow SO_2 + O_2$) at 800° and 850°C. (Plot courtesy of D. Ginosar, Idaho National Lab.)

A novel idea to incorporate Pt into the materials of construction for H_2SO_4 decomposition reaction heat exchanger has been put forth by R. Ballinger [C4]. By adding 1–5 wt% Pt to heat exchanger construction material such as Alloy 800H and Inconel 617, the metals become self-catalytic and the decomposition of H_2SO_4 can be carried without the addition of catalyst pellets. Figure 4-27 shows the micrograph of Alloy 800H alloys with a 2% wt Pt addition. At this low level addition, it has been reported that no change is observable in the alloy but an improvement in the material potential as a catalyst is observed. Development effort is on going to characterize the effectiveness of such alloys for aiding the H_2SO_4 decomposition reaction.

4.13.2. HI Decomposition

The decomposition of HI takes place in the gaseous phase between 300°–450°C depending on the distillation process. Due to the corrosive nature of HI, I_2 and H_2, only a limited number of catalysts have been evaluated in the process. Pt and Pd based catalysts are not suitable as they will exhibit severe corrosion if any measurable amount of moisture is present in the chemical stream. Activated charcoal is the only satisfactory catalyst found to date. However, it has been observed that iodine can be trapped inside

the charcoal pores if the decomposition temperature is too low. Hence, a higher reaction temperature is required in order to maintain the reflux of iodine. Unfortunately, this can lead to accelerated corrosion. There is a need to identify a catalyst that can promote the decomposition at a lower temperature which will be beneficial to the process. There is currently no work on going in this area.

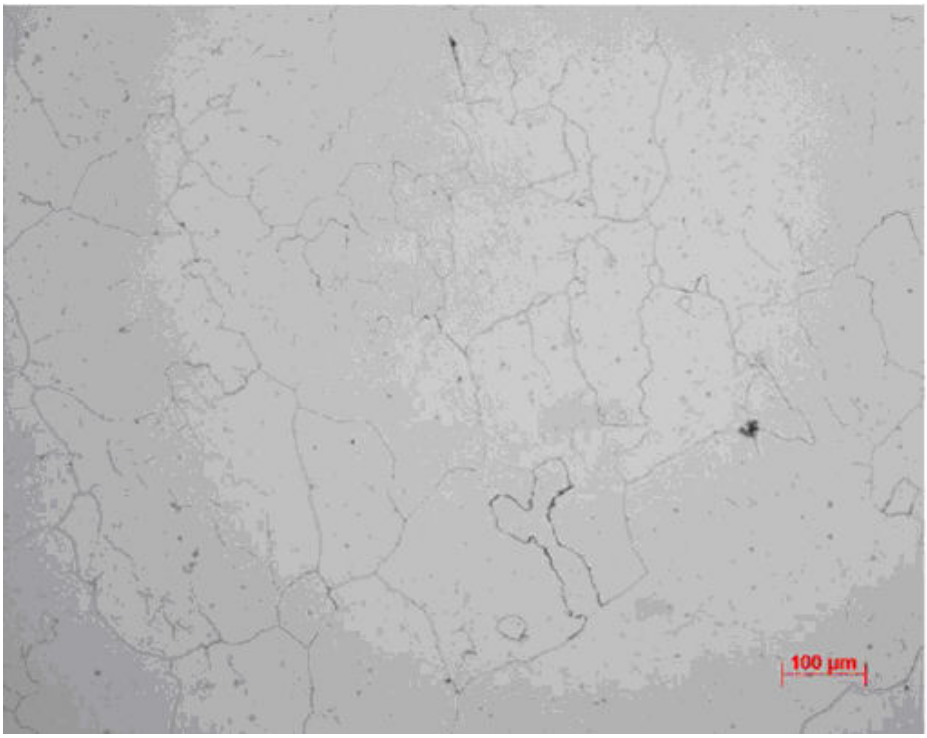

Fig. 4-27. Micrograph of Alloy 800 + 2 wt% Pt at 100X. (Photo courtesy of R. Ballinger, MIT)

4.14. SUMMARY

Commercial success of sulfur-iodine hydrogen production depends largely on the capacity to identify materials of construction that can handle the corrosive environments and on the ability to manufacture process components with these materials economically. This chapter has reviewed a cross section of materials data generated by testing in the various process settings within the cycle. Ta alloys and SiC have been shown to have good corrosion characteristics in all the liquid environments but individual candidate has also been suggested for used for particular condition. Both these materials have unique mechanical properties and much effort is needed in order to use them for component fabrication. In addition, the effect of cross contamination of both process streams and corrosion products on their corrosion performance will need to be addressed. For high temperature sulfur acid decomposition, a number of metallic alloys have been identified but their long term creep characteristics remain an issue. Reactors constructed from SiC

will be undergoing testing in the near term. Even though they are extremely corrosion resistant, obstacles in component fabrication with such ceramic materials remain. Various Hastelloys have demonstrated very good general and stress corrosion behavior in the intermediate temperature HI decomposition environment but the effect of moisture in the vapor stream will need to be studied. Two other important S-I cycle related material areas are separation membrane and catalysts. Different water and hydrogen separation membranes have been investigated. Their long term viability and cost will need to be examined. Pt and oxide based SO_3 decomposition catalysts and their substrates are being studied extensive in an effort to improve their performance. Intelligent designs to incorporate Pt into the decomposer construction materials have shown promises. Similar energy is needed to study HI decomposition catalysts.

4.15. REFERENCES

S-I Cycle General

G1 L.C. Brown, G.E. Besenbruch, R.D. Lentsch, K.R. Schultz, J.F. funk, P.S. Pickard, A. C. Marshal and, S. K. Showalter, "High Efficiency Generation of Hydrogen Fuels Using Nuclear Power," General Atomics Report GA-A24285 Rev. 1 (2001).

G2 J.H. Norman, G.E. Besenbruch, D.R. O'Keefe, "Thermochemical Water-Splitting for Hydrogen Generation," General Atomics Report GA-A15267 (1981) GRI-80/0105.

G3 J.E. Funk, "Thermochemical Hydrogen Production: Past and Present," International Journal of Hydrogen Energy **26**, 185-190 (2001).

G4 L.C. Brown, J.F. Funk, S.K. Showalter, "Initial Screening of Thermochemical Water Splitting Cycles for High Efficiency Generation of Hydrogen Fuels Using Nuclear Power," General Atomics Report GA-A23373 (2000).

G5 K. Onuki, S. Kubo, H. Nakajima, S. Higashi, S. Kasahara, S. Ishiyama, H. Okunda, "R&D on Iodine-Sulfur Thermochemical Water Splitting Cycle at JAERI," JAERI Presentation.

G6 S. Kubo, H. Nakajima, S. Kasahara, S. Higashi, T. Masaki, H. Abe, K. Onuki, "A Demonstration Study on a Closed-Cycle Hydrogen Production by the Thermochemical Water-Splitting Iodine-Sulfur Process," Nucl. Eng. Design **233**, 347-354 (2004).

G7 S. Sato, *Solar-Hydrogen Energy Systems*, Pergamon Press, Oxford (1979) pp. 81-114.

G8 J.H. Norman, K.J. Mysels, D.R. O'Keefe, S.A. Stowell, D.G. Williamson, "Chemical Studies on the General Atomic Sulfur-Iodine Sulfur-Iodine Thermochemical Water-Splitting Cycle," Proceedings of 2nd World Hydrogen Energy Conf., Vol. 2 (1978) p. 513.

G9 J.H. Norman, K.J. Mysels, R. Sharp, D.G. Williamson, "Studies of the Sulfur-iodine Thermochemical Water-splitting Cycle," International Journal of Hydrogen Energy **7**, 545-556 (1982).

G10 B. Russ, "Integrated S-I Laboratory-Scale Experiment Facility Selection," private communication (2006).

G11 Y. Miyamato, *et al.,* "R&D Program on Hydrogen Production System With High-Temperature Cooled Reactor," Presented at International Hydrogen Energy Forum, Munich, Germany, Vol. 2 (2000) pp. 271-278.

G12 H. Ohashi, Y. Inaba, T. Nishihara, Y. Inagaki, T. Takeda, K. Hayashi, S. Katanishi, S. Takada, T. Mano, "Performance Test Results of Mock-up Test Facility of HTTR Hydrogen Production System," Proceedings of the 11th International Conf. of Nuclear Engineering, Tokyo, Japan (2003).

G13 H. Nakajima, M. Sakurai, K. Ikenoya, G.J. Hwang, K. Onuki, S. Shimizu, "Closed Cycle Continuous Hydrogen Production Test by Thermochemical IS Process," Proceedings of the 7th International Conf. on Nuclear Engineering (ICONE-7), Tokyo, Japan (1999).

G14 S. Spewock, L.E. Brecher, F. Talko, "The Westinghouse Sulfur Cycle for the Thermochemical Decomposition of Water," International Journal of Hydrogen Energy **2**, 7-15 (1977).

G15 M. Sakuraia, H. Nakajimaa, R. Amirb, K. Onukia, S. Shimizua, "Experimental Study on Side-Reaction Occurrence Condition in the Iodine-Sulfur Thermochemical Hydrogen Production Process," International Journal of Hydrogen Energy **25**, 613-619 (2000).

G16 Project Staff, "High Pressure Catalytic Metal Reactor in a Simulated Solar Central Receiver," General Atomics Report GA-A18285 (1986).

G17 S. Konche, *et al.,* "Second Law and Cost Analysis of the Oxygen Generation Step of the General Atomic Sulfur–Iodine Cycle," Proceedings of the 5th World Hydrogen Energy Conf., Toronto, Canada, Vol. 2 (1984) pp. 487-502.

G18 M. Sakurai, H. Nakajima, K. Onuki, S. Shimizu, "Investigation of Two Liquid Phase Separation Characteristics on the Iodine-Sulfur Thermochemical Hydrogen Production Process," International Journal of Hydrogen Energy **25**, 605-611 (2000).

G19 M. Roth and K.F. Knoche, "Thermochemical Water Splitting Through Direct HI-decomposition from $H_2O/HI/I_2$ Solutions," International Journal of Hydrogen Energy **14**, 545-549 (1989).

G20 J. Yeheskel, D. Leger, P. Courvoisier, "Thermal Decomposition of Hydriodic Acid and Hydrogen Separation," Advance Hydrogen Energy 2, Vol. 1 (1979) p. 569

G21 S. Kasahara, G.J. Hwang, H. Nakajima, H.S. Choi, K.M. Onuki, "Effects of Process Parameters of the IS Process on Total Efficiency to Produce Hydrogen from Water," Journal of Chemical Egg. Japan **36**, 887-899 (2003).

Materials of Construction

M1 P.W. Trester and H.G. Staley, "Assessment and Investigation of Containment Materials for the Sulfur-Iodine Thermochemical Water-Splitting Process for Hydrogen Production," Gas Research Institute Report GRI-Report 80/0081 (1981).

M2 Project Staff "Decomposition of Sulfuric Acid Using Solar Thermal Energy," General Atomics Report GA-A17573 (1985).

M3 P.W. Trester and S.S. Liang,, "Material Corrosion Investigations for the General Atomic Sulfur-Iodine Thermochemical Water-Splitting Cycle," Proceedings of the Second World Hydrogen Energy Conference, Zurich, Switzerland, 1978, Pergamon Press, Vol. 4. (1979) pp. 2113-2159.

M4 S. Kubo, H. Nakajima, S. Higashi, K. Onuki, S. Shimizu, N. Akino, "Construction of Apparatus for Thermochemical Hydrogen Production Process," Proceedings of the 11th Canadian Hydrogen Conf., Vol. 5A (2001)

M5 S. Kubo, *et al.,* "Corrosion Test on Structural Materials for Iodine-Sulfur Thermochemical Water-Splitting Cycle," Proceedings of the 2nd Topical Conf. on Fuel Cell Technology, AIChE 2003 Spring National Meeting (2003).

M6 K. Onuki, I. Ioka, M. Futakawa, H.Nakajima, S. Shimizu, and I. Tayama, "Screening Tests on Materials of Construction for the Thermochemical IS Process," Corrosion Engineering **46**, 141-149 (1997).

M7 K. Sugahara, Y. Takizawa, E. Akiyama, and K. Hashimoto, "The Corrosion Behavior of Ni-Cr-Mo Ternary Alloys in Hot Concentrated Sulfuric Acid with Active Carbon (Part 1)," Corrosion Engineering **46**, 773-783 (1997).

M8 T. Lillo, "Materials for the Sulfuric Concentration and Decomposition Section," Idaho National Laboratory private communication (June 2005).

M9 Y. Kurata, K. Tachibana and T. Suzuki, "High Temperature Tensile Properties of Metallic Materials Exposed to a Sulfuric Acid Decomposition Gas Environment," J. Japan Inst. Metals **65**, 262-265 (2001).

M10 F. Porisini, "Selection and Evaluation of Materials for the Construction of a Pre-Pilot Plant for Thermal Decomposition of Sulfuric Acid," International Journal on Hydrogen Energy **14**, 267-274 (1989).

M11 F. Porisini, "Corrosion Resistance of Si-Containing Ni-Fe-Cr Alloys Used as Materials for the Thermal Decomposition of Sulfuric Acid," International Journal on Hydrogen Energy **10**, 255-262 (1985).

M12 F. Porisini, "Long Term Corrosion Tests of Materials for Thermal Decomposition of Sulfuric Acid," International Journal on Hydrogen Energy **8**, 819-828 (1983).

M13 E.M. Savitsky, E.P. Arskaya, E.M. Lazarev and N.A. Korotkov, "Investigation of Corrosion Resistance of Materials in the Presence of Sulfuric Acid and Its Decomposition Products Applied in the Thermochemical Cycle of Hydrogen Production," International Journal on Hydrogen Energy 7, 393-396 (1982).

M14 *Handbook of Corrosion Data*, Ed. B.D. Craig, ASM International, Metals Park, Ohio (1989).

M15 G.Y. Lai, *High-Temperature Corrosion of Engineering Alloys*, ASM International, Materials Park, Ohio (1990).

M16 A. Robin and J.L. Rosa, "Corrosion Behavior of Niobium, Tantalum and Their Alloys in Hot Hydrochloric and Phosphoric Acid Solutions," International Journal of Refractory Metals and Hard Mater. **18**, 13-21 (1997).

M17 A. Robin, "Corrosion Behavior of Niobium, Tantalum and Their Alloys in Boiling Sulfuric Acid Solutions," International Journal of Refractory Metals and Hard Materials **15**, 317-323 (1997).

M18 F.H. Gern and R. Kochendoerfer, "Liquid Silicon Infiltration: Description of Infiltration Dynamics and Silicon Carbide Formation," Composites Part A **28A**, 355-364 (1997).

M19 B. Wong, L.C. Brown and G.E. Besenbruch, "Corrosion Screening of Construction Materials for Hydrogen Iodide Decomposition Heat Exchanger Fabrication," General Atomics Report GA-A25128 (2005).

Membranes

T1 F.F. Stewart, C.J. Orme, and M.G. Jones, "Membrane Processes for the Sulfur-Iodine Thermochemical Cycle," AIChE Spring Meeting, 2005, Atlanta.

T2 G.J. Hwang, K. Onuki, and S. Shimizu, "Separation of Hydrogen from a H_2 - H_2O- HI Gaseous Mixture Using a Silica Membrane," AIChE **46**, 92 (2000).

T3 C.J. Orme, M.G. Jones, F.F. Stewart, "Pervaporation of Water from Aqueous HI Using Nafion-117 Membranes for the Sulfur-Iodine Thermochemical Water Splitting Process," Journal of Membrane Science **252**, 245-252 (2005).

T4 M. Nomura, S. Fujiwara, K. Ikenoya, S. Kasahara, H. Nakajima, S. Kubo, G.-J. Hwang, H.-S. Choi, K. Onuki, "Application of an Electrochemical Membrane Reactor to the Thermochemical Water Splitting IS Process for Hydrogen Production," Journal of Membrane Science **240**, 221–226 (2004).

T5 M. Nomura, S.-I. Nakao, H. Okuda, S. Fujiwara, S. Kasahara, K. Ikenoya, S. Kubo, K. Onuki, "Development of an Electrochemical Cell for Efficient Hydrogen Production Through the IS Process," Environment and Energy Engineering **50**, 1991-1998 (2004).

T6 G.-J. Hwang, K. Onuki, M. Nomura, S. Kasahara, J.-W. Kim, "Improvement of the Thermochemical Water-Splitting IS (Iodine-Sulfur) Process by Electro-Electrodialysis," Journal of Membrane Science **220**, 129-136 (2003).

T7 Y. Yoshino, T. Suzuki, B.N. Nair, H. Taguchi, an N. Itoh, "Development of Tubular Substrates, Silica Based Mmembranes and Membrane Modules for Hydrogen Separation at High Temperature," Journal of Membrane Science **267**, 8-17 (2005).

T8 G.-J. Hwang, K. Onuki, M. Nomura, S. Kasahara, J.-W. Kim, "Improvement of the Thermochemical Water-splitting IS (iodine-sulfur) Process by Electro-electrodialysis," Journal of Membrane Science **220**, 129-136 (2003).

T9 G.J. Hwang and K. Onuki, "Simulation Study on the Catalytic Decomposition of Hydrogen Iodide in a Membrane Reactor With a Silica Membrane for the Thermochemical Water Splitting IS Process," Journal of Membrane Science **194**, 207 (2001).

T10 M. Nomura, S. Kasahara, H. Okuda, S.-I. Nakao, "Evaluation of the IS Process Featuring Membrane Techniques by Total Thermal Efficiency," International Journal of Hydrogen Energy **30**, 1465-1473 (2004).

T11 M. Nomura, K. Ono, S. Gopalakrishnan, T. Sugawara and S.-I. Nakao, "Preparation of a Stable Silica Membrane by a Counter Diffusion Chemical Vapor Deposition Method," Journal of Membrane Science **251**, 151-158

(2005).

T12 G.-J. Hwang, J.-W. Kim, H.-S. Choi and K. Onuki, "Stability of a Silica Membrane Prepared by CVD Using and Alumina Tube as the Support Tube in the HI–H_2O Gaseous Mixture," Journal of Membrane Science **215**, 293–302 (2003).

Catalysts

C1 D.M. Ginosar, A.W. Glenn and L.M. Petkovic, "Stability of Sulfuric Acid Decomposition Catalysts for Thermochemical Water Splitting Cycles," AIChE Spring Meeting, 2005, Atlanta.

C2 H. Ishikawa, E. Ishii, I. Uehara, and M. Nakan, "Catalyzed Thermal Decomposition of H_2SO_4 and Production of HBr by the Reaction of SO_2 With Br_2 and H_2O," International Journal for Hydrogen Energy **46**, 237-246 (1982).

C3 H. Tagawa and T. Endo, "Catalytic Decomposition of Sulfuric Acid Using Metal Oxides as the Oxygen Generating Reaction in Thermochemical Water Splitting Process," International Journal of Hydrogen Energy **14**, 11-17 (1989).

C4 R. Ballinger, "The Development of Self-Catalytic Materials for Thermochemical Water Splitting Using the Sulfur-Iodine Process," Presentation at the UNLV-HTHX Quarterly Meeting, University of Las Vegas, Las Vegas, Nevada, December 2005.